**Title**

A fruit pick-up mechanism for reducing dust generation in almond pick-up machines



**Author**

Serajian, Reza

**Publication Date**

2023

UNIVERSITY OF CALIFORNIA, MERCED

# A FRUIT PICK-UP MECHANISM FOR REDUCING DUST GENERATION IN ALMOND PICK-UP MACHINES

by

Reza Serajian

A thesis submitted in partial satisfaction of the
requirements for the degree of
Doctor of Philosophy

in

Mechanical Engineering

Committee in charge:
Professor Reza Ehsani, Chair
Professor Jian-Qiao Sun
Professor Jeanette Cobian-Iñiguez
Professor Ricardo Pinto de Castro

The thesis of Reza Serajian is approved:

| | |
|---|---|
| Reza Ehsani, Chair | Date |
| Jian-Qiao Sun | Date |
| Jeanette Cobian-Iñiguez | Date |
| Ricardo Pinto de Castro | Date |

University of California, Merced

To my lovely parents.

## ACKNOWLEDGEMENTS

I would like to express my deepest gratitude to those who have made this journey not only possible but also a memorable and enriching experience.

First and foremost, I extend my heartfelt thanks to my parents, my sister, and my two brothers. Their unwavering mental and soulful support has been the cornerstone of my journey. Their belief in me, even in times of challenge, has been a source of strength and inspiration, for which I am eternally grateful. The support and understanding from my siblings have been invaluable, providing a foundation of familial love and encouragement that has buoyed me throughout this process.

I am also profoundly grateful to Bahar, whose unconditional love has been a guiding light through this endeavor. Her presence in my life has brought joy and a sense of purpose that goes beyond words. Bahar, your love has been a constant reminder of the beauty and goodness in the world.

Additionally, I want to acknowledge Chaly for the love and kindness bestowed upon me. The warmth and care received have been a source of comfort and encouragement. In times of stress and deadlines, this kindness has been a sanctuary, reminding me of the importance of compassion and humanity.

This journey has been made brighter and more meaningful because of all of you. Your love and support have been my pillars of strength. I am deeply grateful for everything.

# CURRICULUM VITAE

## Education

B.S. in Railway Rolling Stock, Iran University of Science and Technology (Tehran, Iran)

M.S. in Mechanical Engineering, University of California, Riverside (Riverside, USA)

## Honors

Dean's Distinguished Fellowship, Riverside, USA (2015-2017), University of California, Riverside.

California Non-resident tuition and fees, Merced, USA (2018), University of California at Merced.

Grand Award Judge (INTEL, ISEF), Los Angeles, USA(2017)

First ranked Student in School of Railway Eng., Tehran, Iran (2005)

## Publications

R. Serajian, J.Q. Sun, and R. Ehsani (2023): "Design of an Integrated Controller for a Sweeping Mechanism of a Low-Dust Almond Pickup Machine". *Sensors.* 23(4), 2046. https://doi.org/10.3390/s23042046

R. Serajian et al. (2023): "Freight train air brake models". *International Journal of Rail Transportation.*
11(1), 1-49.https://doi.org/10.1080/23248378.2021.2006808

R. Serajian and R.Ehsani (2020): "Application of big data for improving air quality during almond harvesting process". *2020 IEEE International Conference On Big Data (Big Data). Atlanta, GA, USA.* 5819-5821.DOI: 10.1109/BigData50022.2020.9377820

R. Serajian, S. Mohammadi, and A. Nasr (2019): "Influence of train length on in-train longitudinal forces during brake application". *Vehicle system dynamics.* 57(2), 192-206. https://doi.org/10.1080/00423114.2018.1456667

S. Mohammadi, R. Serajian (2015): "Effects of the change in auto coupler parameters on in-train longitudinal forces during brake application". *Mechanics & Industry.* 16(2), 1-13. DOI:10.1051/meca/2014073

R. Serajian (2013): "Parameters' changing influence with different lateral stiffnesses on nonlinear analysis of hunting behavior of a bogie". *Journal of Measurements in Engineering*. 1(4), 195-206

D Younesian, AA Jafari, and R Serajian (2011): "Effects of the bogie and body inertia on the nonlinear wheel-set hunting recognized by the hopf bifurcation theory". *Internationa Journal of Automotive Engineering*. 1(3), 186-196

# TABLE OF CONTENTS

# LIST OF FIGURES

# LIST OF TABLES

# ABSTRACT

This doctoral research addresses a critical environmental challenge in California's almond orchards: the pervasive dust pollution stemming from traditional almond harvesting methods. As the leading producer of almonds, supplying over 80 percent of the global demand, California has long been confronted with the adverse effects of these practices on air quality and health, notably the substantial emissions of particulate matter (PM), particularly PM2.5 and PM10. At the core of my study was the conception, design, and iterative development of an innovative low-dust sweeping system aimed at drastically reducing dust emissions during almond harvesting. This journey involved the creation and successive refinement of ten distinct versions of the machine, each iteration addressing limitations and inefficiencies identified in its predecessor. This meticulous process of design and modification was pivotal in evolving the system to its final form, incorporating a sophisticated feedback control mechanism that intelligently adjusts the sweeper brushes' height and speed in synchrony with the harvester's movement. This innovation significantly refined the interaction between the brushes and the ground, reducing unnecessary sweeping and, as a result, mitigating dust generation. Comparative field tests with conventional harvesting equipment from renowned brands like Flory, Weiss McNair, and Jack Rabbit in Fresno County orchards established that our final low-dust model, encapsulating the refinements from previous versions, notably outperformed its predecessors in minimizing PM emissions. Furthermore, this research made a significant stride in predicting PM2.5 emissions, a previously unaddressed challenge in California's almond industry. The absence of a reliable emission factor for PM2.5 has been a significant barrier to regulatory compliance and emissions inventory. The predictive model developed as part of this research is a substantial contribution toward understanding and managing the environmental impact of almond harvesting operations. In conclusion, the final version of the low-dust almond harvesting system developed through this research not only meets but surpasses California's air quality standards. It offers an effective, environmentally responsible solution for the almond industry, embodying the essence of sustainable innovation and marking a significant step forward in harmonizing agricultural efficiency with environmental stewardship.

# Chapter 1

# ALMOND HARVESTING AND AIR QUALITY IMPACT

## 1.1 Introduction

450,000 acres in San Joaquin Valley in California are used for growing almonds. Almond is the largest tree nut crop in total $ value. California grows %80 of the whole world's crop and it is the 7th largest US food export. There are 6000 almond growers in California, and around 90 nations are importing CA almonds. In Figure 1.1, almond production acreage data by USDA report shows growth in almond production in California. It implies that agricultural land in 2020 for almonds has increased by around 3.5 times in comparison with the land in 1996.

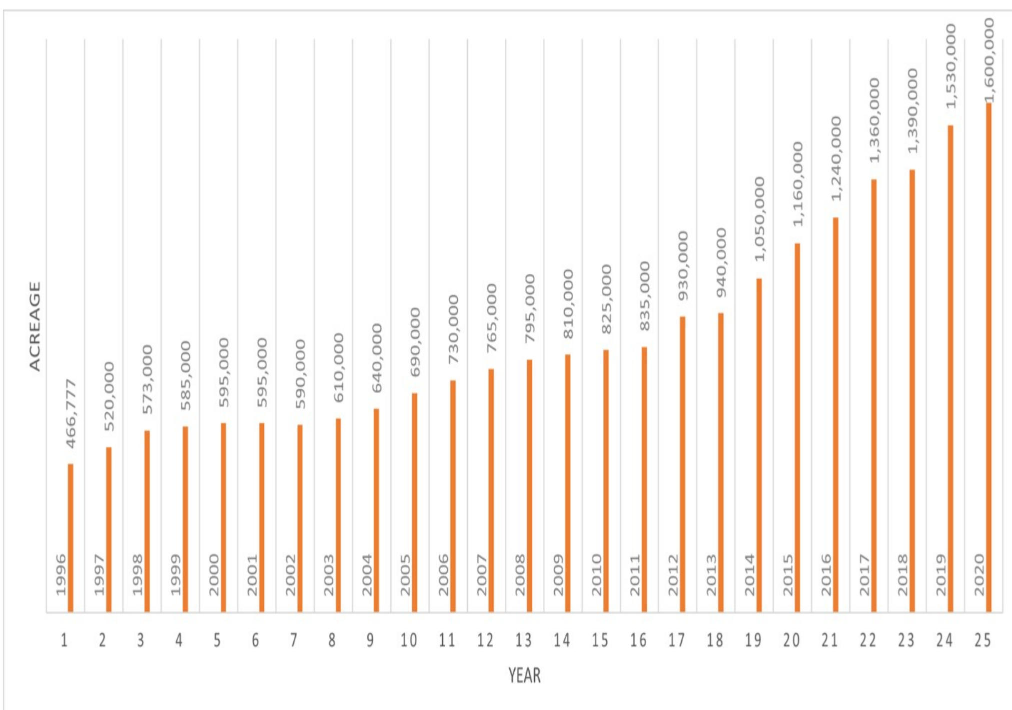


Figure 1.1: California almond acreage by USDA[1]

In Table 1, almond production in million pounds, and the value of production in dollars are listed from 1995 to 2021. This table also shows how beneficial almond production is for California as a business industry. The value of almond production has increased about 7 times in the past 25 years which is now 5.6 billion dollars. By applying scientific methods for planting and growing almond, yield per acre also has increased significantly which shows almond production is becoming more in both yield per acre and value. float

Table 1.1: California Almond Acreage, Production, and Value: 1995-2022 [2]

| **Year** | **Acre** | **Pound/Acre** | **Prod. (Mil. lbs)** | **$/Pound** | **Value ($1K)** |
|---|---|---|---|---|---|
| 1995 | 483,700 | 890 | 370 | 2.48 | 880,896 |
| 1996 | 500,400 | 1,190 | 510 | 2.08 | 1,018,368 |
| 1997 | 520,000 | 1,720 | 759 | 1.56 | 1,160,640 |
| 1998 | 573,000 | 1,130 | 520 | 1.41 | 703,590 |
| 1999 | 585,000 | 1,720 | 833 | 0.86 | 687,742 |
| 2000 | 595,000 | 1,380 | 703 | 0.97 | 666,487 |
| 2001 | 605,000 | 1,570 | 830 | 0.91 | 740,012 |
| 2002 | 610,000 | 2,000 | 1,090 | 1.11 | 1,200,687 |
| 2003 | 610,000 | 1,890 | 1,040 | 1.57 | 1,600,144 |
| 2004 | 640,000 | 1,760 | 1,005 | 2.21 | 2,189,005 |
| 2005 | 700,000 | 1,550 | 915 | 2.81 | 2,525,909 |
| 2006 | 755,000 | 1,840 | 1,120 | 2.06 | 2,258,790 |
| 2007 | 765,000 | 2,170 | 1,390 | 1.75 | 2,401,875 |
| 2008 | 825,000 | 2,300 | 1,630 | 1.45 | 2,343,200 |
| 2009 | 840,000 | 1,880 | 1,410 | 1.65 | 2,293,500 |
| 2010 | 855,000 | 2,130 | 1,640 | 1.79 | 2,903,380 |
| 2011 | 875,000 | 2,540 | 2,030 | 1.99 | 4,007,860 |
| 2012 | 930,000 | 2,310 | 1,890 | 2.58 | 4,816,860 |
| 2013 | 1,000,000 | 2,280 | 2,010 | 3.21 | 6,384,690 |
| 2014 | 1,100,000 | 2,010 | 1,870 | 4 | 7,388,000 |
| 2015 | 1,190,000 | 2,000 | 1,900 | 3.13 | 5,868,750 |
| 2016 | 1,270,000 | 2,210 | 2,140 | 2.39 | 5,052,460 |
| 2017 | 1,360,000 | 2,200 | 2,270 | 2.53 | 5,603,950 |
| 2018 | 1,390,000 | 2,090 | 2,280 | 2.5 | 5,602,500 |
| 2019 | 1,530,000 | 2,160 | 2,550 | 2.45 | 6,169,100 |
| 2020 | 1,600,000 | 2,490 | 3,115 | 1.71 | 5,619,930 |
| 2021 | 1,640,000 | 2,210 | 2,915 | 1.76 | 5,028,320 |
| 2022 | 1,630,000 | 1,900 | 2,565 | 1.4 | 3,515,400 |

### 1.2 Almond harvesting steps

Two weeks after the last irrigation for almonds, between mid-August and October, almond harvesting occurs. Before it happens, weeds and other debris and branches should be removed from the orchard floor. Specialized harvesting pieces of machinery are used for shaking trees in order to drop almonds to the ground, which is a kind of dusty job, but dry conditions are more important than anything to reducing mold and bacterial contamination of the almonds. When the nuts are ready, pickup machines pick up the nuts from the ground and convey them into carts or trailers that are used to transport the almonds to the huller/sheller.


Figure 1.2: Almond harvesting steps (a. shaking, b. sweeping, c. pick up, c. pick up) [3, 4, 5]

### 1.3 Harvest dust impact

Shaking almond trees generates %11 of all dust emissions in the harvesting process, sweeping %13 and picking up %76. In general, the almonds pickup process is the main source of dust generation which should be controlled to avoid its negative effects on the environment and people's health. Increased acreage of almond production in California over the last few years resulted in increased emission of dust pollution during harvest, which could result in the following effects:

- Highly visible and localized particulate emissions during harvest.
- Negative impact on neighbor communities, roads, and nearby highways.
- Receiving a significant number of fugitive dust complaints by the district.

To address this issue, particulate matter (PM) needs to be reduced in rural areas to reduce localized impacts on communities and nearby highways.

### 1.4 Particulate Matter (PM)

Solid or liquid particles found in the atmosphere are known as particulate matter (PM), particulates, or particle pollution. They are in different sizes, and the smaller the particles, the more easily and deeply they can enter our lungs and cause health problems. These tiny particles may bring about problems like difficulty in breathing and sometimes permanent lung damage. Affecting the heart and causing palpitations and chest pain are other possible issues caused by these small particles. The most sensitive people to particle pollution are children, older adults, and people with heart or lung disease. Figure 1.3 shows different particulate matter sizes. PM10 is the one with a spherical diameter equal to or less than 10 micrometers, and PM2.5 has diameters equal to or less than 2.5 microns. Both types of PMs mentioned are inhalable and PM2.5 can directly go to the human bloodstream.

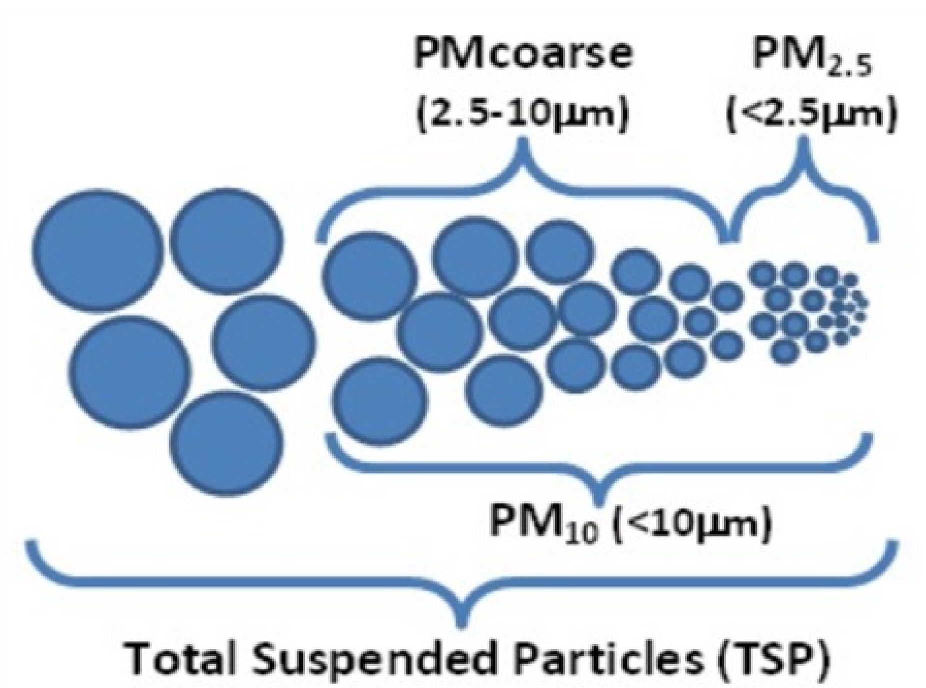


Figure 1.3: Particulate matter sizes [6]

Figure 4 visually illustrates the comparison between PM10, PM2.5, beach sand, and human hair. Indicating how small they are and why so easily they can get into our body.

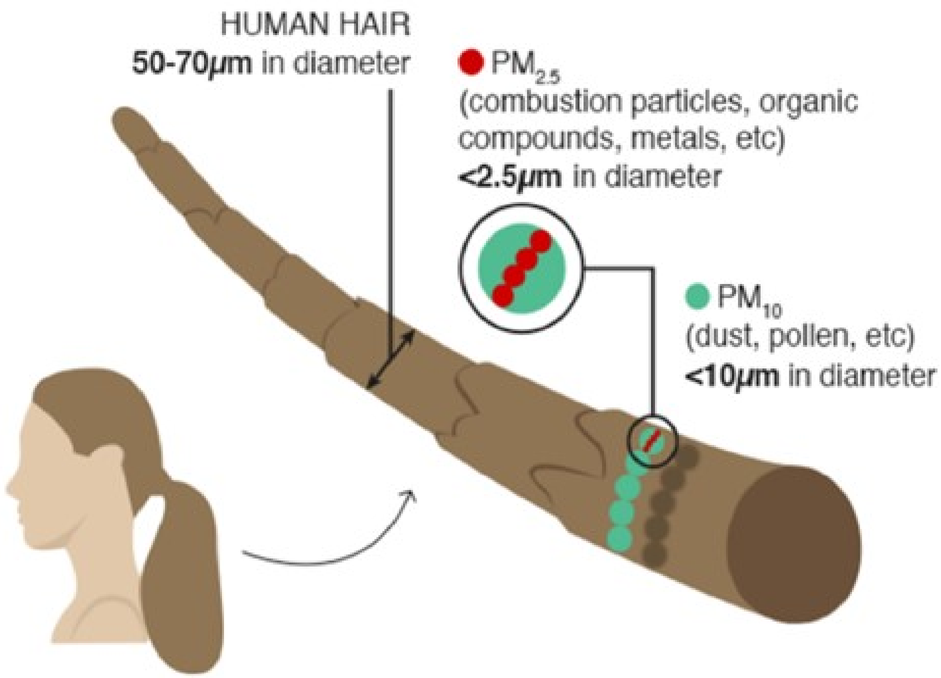


Figure 1.4: Comparison of the relative size of particle matters to a human hair [6]

### 1.5 Health and environmental effects of particulate matter (PM)

Tiny particulate matter can harm both your lungs and your heart if you are exposed to them. Particle pollution has been linked in many scientific studies to several issues, including:

- Early death in those with heart or lung disease
- Nonfatal heart attacks
- Irregular heartbeat
- Aggravated asthma
- Decreased lung function
- increased respiratory symptoms, such as irritation of the airways, coughing or difficulty breathing.

These undesirable health effects are most likely to occur in children, older adults, and people with lung or heart problems.

## 1.6 Federal and state ambient air quality standards (NAAQS) for PM

The maximum amount of pollution that can be present in outdoor air without endangering human health is defined by ambient air quality guidelines. In Table 1.2, both federal and state mandates for particulate matters are shown, which should be followed by all industries, including the agricultural industry, by 2025.

Table 1.2: Federal and California state ambient air quality standards for PM2.5 and PM10[7]

| **Ambient Air Quality Standard** | **PM2.5** | | **PM10** | |
|---|---|---|---|---|
| | Annual avg | 24-hour avg | Annual avg | 24-hour avg |
| **Federal** | 12 µg/m3 | 35 µg/m3 | None | 150 µg/m3 |
| **California State** | 12 µg/m3 | None | 20 µg/m3 | 50 µg/m3 |

Environmental Protection Agency measures dust as PM10. It comprises particles of residue or ash that are 10 microns in size or smaller. The more destructive PM2.5 is a subset of PM10 and can regularly be associated with half of any PM10 estimation. Any industry should be in compliance with the government standard for residue, or PM10, which is 150 micrograms found the middle value of more than 24 hours, which also is mandated by the state to be 50 micrograms per cubic meter in 24 hours. In Figure 5, the average PM10 during months when almonds are not harvested is displayed, while in Figure 6, the average PM10 is shown in harvested almond months. We clearly see that the increase in PM10 contamination due to agricultural activities (Almond harvesting) is a concern that should be controlled.

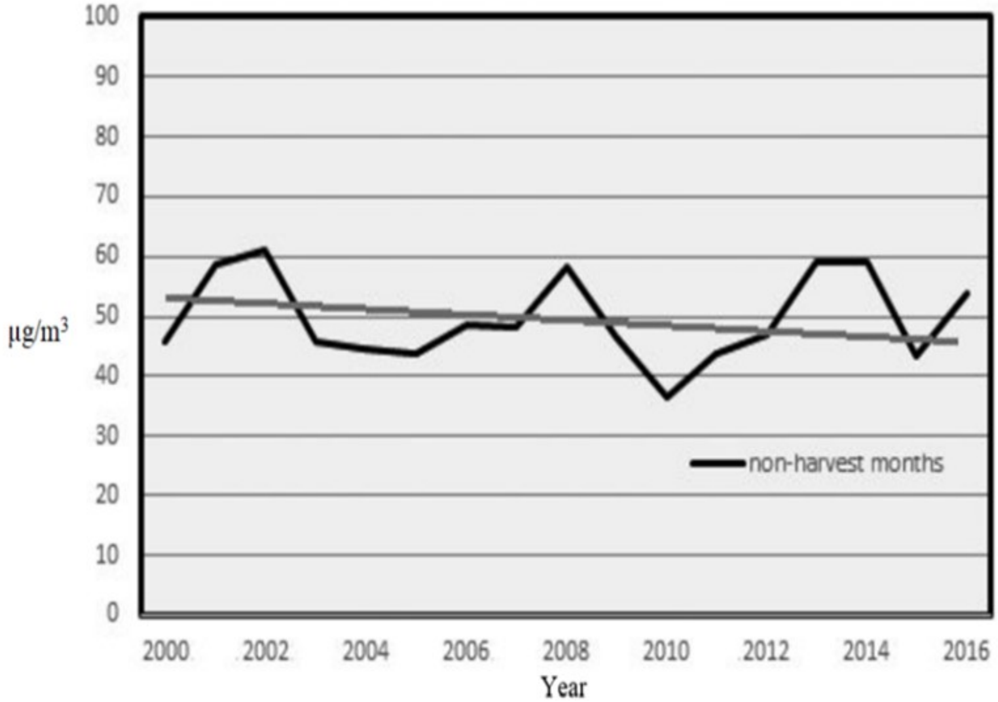


Figure 1.5: PM10 average during months when almonds are not harvested [8]

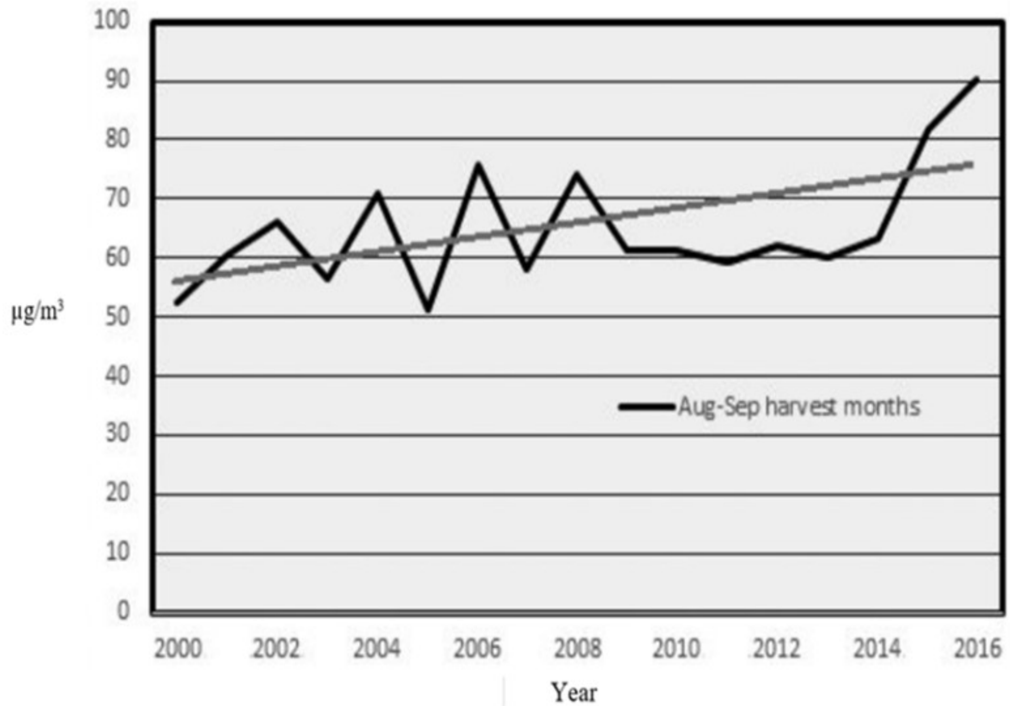


Figure 1.6: PM10 average during months when almonds are harvested [8]

## 1.7 Literature review

### 1.7.1 Commercial low-dust almond harvesters

There have been several attempts by the manufacturers of almond harvesting equipment to modify their equipment to reduce dust during the pickup process. What they focused on was reducing dust after the pickup step in their machines while transferring almonds into the hopper to accumulate crops. A manufacturer called "Exact Corporation" tried to trap dust in a container with a spinning brush in it and inject water into the generated dust. It could help reduce dust, but it made more problems like maintenance requirements for removing the mud that was generated in the container. Refilling water to spray over the dust was another issue that could slow down the process. Flory Industries attempted making the conveyor belt transfer almonds to the hopper longer to get rid of dust slower and reduced fan speed for removing debris and leaves, but this producer could not achieve much in dust reduction because this could just eliminate a small portion of the dust. Jackrabbit Corporation designed a disk-based cleaning section to separate dust from almonds and Molded resin discs which were replaced with a metal cleaning chain that could fall out more dirt, but big size sands. All these activities are done in low-dust harvesters after too much dust is already generated in pickup action. This will consume more energy if the harvester generates dust first, and new designs try to eliminate that dust. Figure 1.7 visually illustrates that the modified almond pickup system still generates a significant amount of dust during the pickup process. This depicts the necessity of designing a new version of the pickup system to help reduce the dust significantly for have a safe atmosphere for people living in the area.

Table 1.3: Most recent commercial low-dust almond harvesters

| **Manufacturer** | **Model** | **Drive** | **Technology notes** |
|---|---|---|---|
| **Harvester pickup equipment** | | | |
| Exact Corporation | E-3800 | Pull-behind PTO | Features a water misting and brush system at the separation fan. Reduced discharge airspeed |
| | E-4000 | Pull-behind PTO | |
| | E-7000SP | Self-Propelled | |
| Flory Industries | 860 XL | Pull-behind PTO | Reduced fan speed, longer cleaning chain length, and changes to location of dust discharge. Reduced discharge airspeed. |
| | 8600 XL | Self-Propelled | |
| | 8770 XL | Self-Propelled | |
| Jackrabbit | Harvester | Pull-behind PTO | Disk-based cleaning section, with twin-rod out load chain. Adjustable fan speed and damper. |
| Weiss-McNair | 9800 California Special | Pull-behind PTO | Reduced fan speed, fan location, enlarged vacuum and separation chambers, and cleaning chain design. Reduced discharge airspeed. |
| | Magnum X | Self-Propelled | |
| **Shaker/Sweeper combination unit** | | | |
| Tenias | Almond Harvester | Self-Propelled | Shaker drops nuts onto a plate and funnels them into windrows; eliminates the need for the sweeping process (sweeper/shaker in one combined unit) |


Figure 1.7: Commercial low-dust harvesters[9, 10, 11, 12]

## 1.8 Project aim

The ultimate goal of this study is to develop a new, highly energy-efficient almond pickup system that produces minimal or zero dust. This research focuses on preventing dust generation from the outset rather than managing high volumes of dust after generation.

## 1.9 Objectives

- To integrate sweeping and pickup steps into a singular, efficient process for almond harvesting.
- To design and engineer an optimal mechanism for almond sweeping and pickup, prioritizing the minimization of dust generation.
- To develop an automated feedback control system, aimed at maximizing the efficiency of almond sweeping from the ground while minimizing dust generation through reduced soil contact.
- To apply predictive neural network modeling, using operational data to estimate dust generation and facilitate real-time adjustments for optimal dust control.

- To conduct comparative performance evaluations of the designed almond pickup and sweeper systems against existing commercial machines, emphasizing their effectiveness in reducing dust emissions.

# Chapter 2

# EVOLUTIONARY DESIGN AND METHODOLOGY OF ALMOND PICKUP MACHINES

## 2.1 Introduction

I began this project in the summer of 2019, during which time I embarked on a journey of designing, manufacturing, and testing various iterations of the machine. This process culminated in a final, refined version. In this section, I will provide a concise overview of each prototype developed, highlighting the challenges encountered during the pickup process. This narrative will offer readers a clearer understanding of the evolution and optimization of the design.

## 2.2 Method for the combination of sweeping and pickup steps

### 2.2.1 First Design - Exploring the adaptation of pinwheel technology for almond collection

In this design, we tried to evaluate if the pinwheel technology used to pick up macadamia- can be adapted to existing pickup systems or not. (Macadamia is largely grown in Australia with grassy and dense orchards). For this, the first step was to give the system flexibility to be able to move forward for any bumpy orchard. While moving forward, flexible pins grab the nut, and it gets ejected by fixed rods located at the top of the rotating green wheels. When it gets out of the pin, it falls into the horizontal auger to be transferred for accumulation. We tested this version in a real almond orchard and no dust was generated, but this system was able to pick only the top layer of the crop on the floor and needed more passes to take all the nuts. The other problem was large branches meeting spinning wheels and stopping some of them from spinning. This prototype and the result of the pickup tests are displayed in Figures 2.1to 2.3.

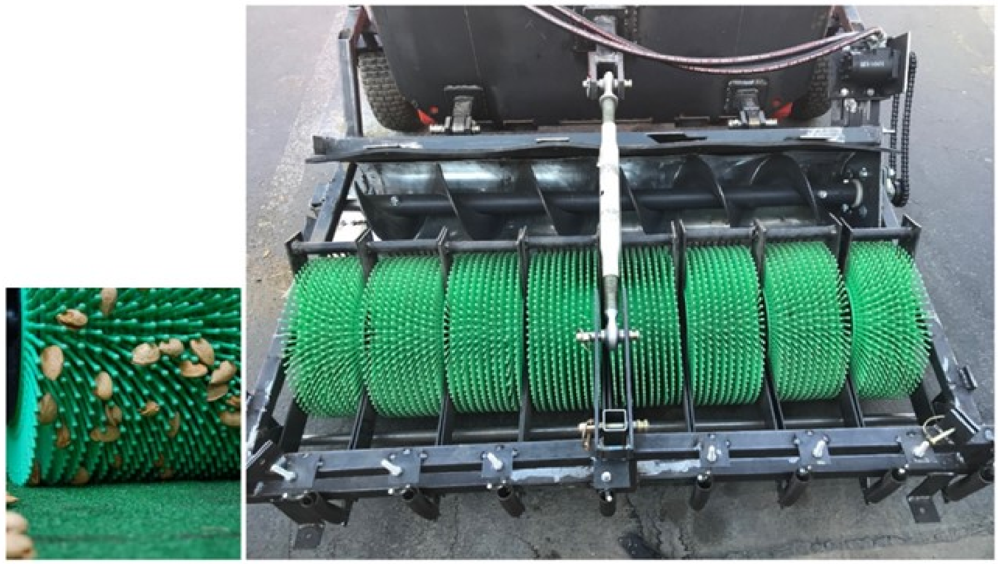

Figure 2.1: First new version low-dust pickup machine design

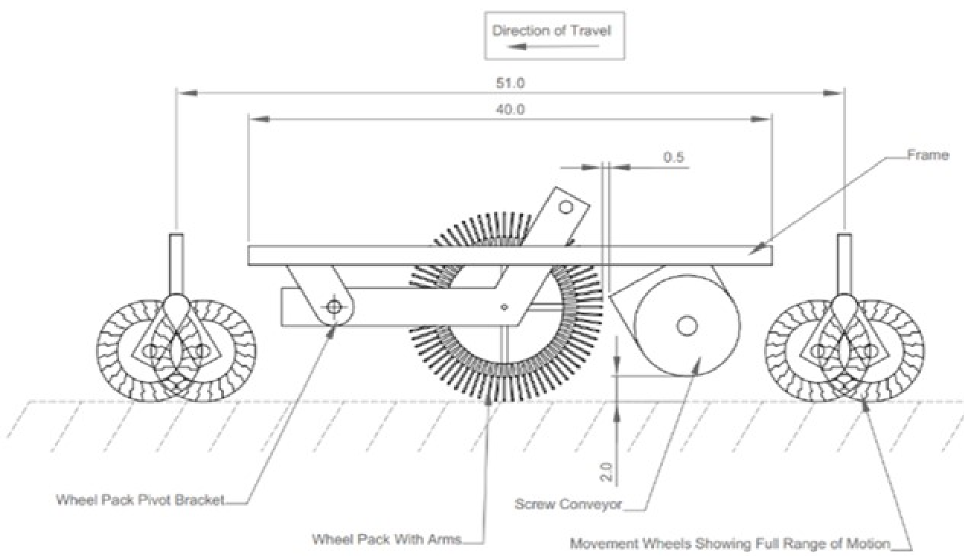


Figure 2.2: Schematic of the first design

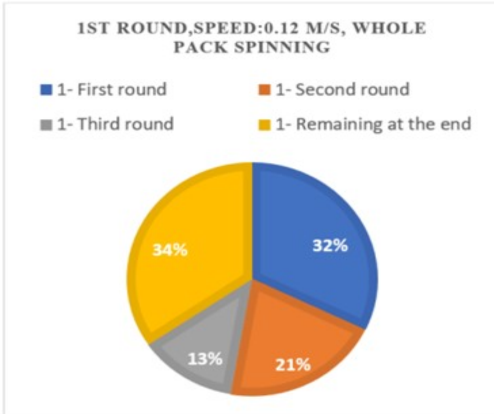


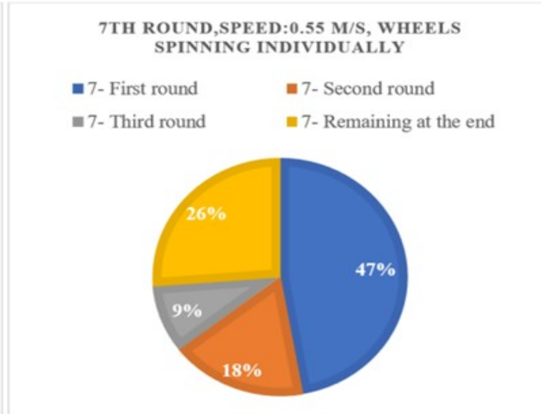


Figure 2.3: Pickup rate and remaining almond with different speeds for 1st design

### 2.2.2 Second Design - Enhancing Collection with Targeted Brushing (Refinements to direct almond collection using added brushes.)

In this design, we needed to target most of the almonds fallen on the floor into the front part of the pickup system, so we added a brush to guide crops in front of the spinning pinwheels. This caused a little dust and brush modification was needed. The efficiency of the system increased in this design, but a thick rubber brush dug into the floor and generated dust. This was a good achievement that after three passes, no almond was on the floor, but our goal was picking up in just one pass. The manufactured design and test results are shown in Figures 2.4 and 2.5.

Figure 2.4: Second design with low-speed rubber brush

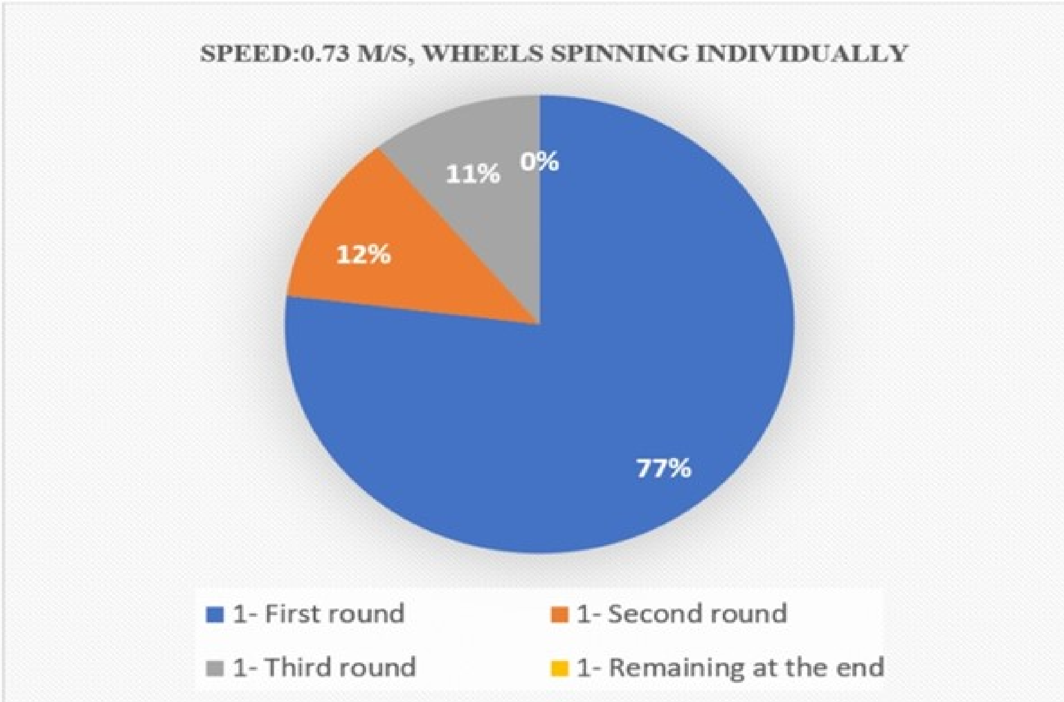


Figure 2.5: Pickup rate and remaining almond for 2nd design

### 2.2.3 Third Design - Transition to Rubber Brushes and Plate Adjustments

In the second modification for the third design, according to the problems raised with the pinwheel system, we decided to remove them and do the sweeping and pick-up with rubber brushes. These brushes could work well, but at high speeds, bent up and could not touch the nut. Floating concave plates were used in the bottom of the brushes to move smoothly on the dust, which would not dig into the floor.

Figure 2.6: Third design with two brushes and concave plates

### 2.2.4 Fourth Design - Advancements in Brush Design and Hydraulic Motor Integration for uneven orchard terrain

In this modification, a new model for the brush was designed, which uses plastic tines that are fixed in an inclined way to touch nuts smoothly and not dig into the floor. The problem seen in this design was the change of the brush elevation due to bumps contacts with the bottom part of the plates. Any pressure acting from the floor could bend the whole rotating system and decrease the pickup efficiency. The gap between the tines and the floor is suggested to be half an inch which is smaller than the smallest size of an average almond. With this, every nut would be hit by brushes. The other innovation in brush designing was to rotate brush plates about two perpendicular axes to meet the ground only for 100 degrees in front of the moving machine. In this design, useless ground touch is removed, and lower dust would be generated. Still, the concave plates' bending problem existed and should have been resolved. In this modification, hydraulic motors were used which could be run by moving the machine's hydraulic power. It was working well just in flat orchards. More modifications were required for using our system in different types of orchards with floor level changes. Fourth design with new brushes and modified brush-floor gap.

### 2.2.5 Fifth Design - Electrifying the Sweeping Process (Transitioning to an electrically powered brushing system for increased efficiency)

Controlling the brush from the top with an electrical motor which uses the moving vehicle's electrical energy for running represented a very light brushing system (15 lb.) instead of the brushing system in the 4th version with heavy hydraulic motors (100 lb. each) was a valuable achievement in this version. We tested it and saw that the brushing system works properly and can sweep 100% of the crop. The only concern for the brushing system was controlling the height and spinning speed. In the final version, by adding an actuator to the system and using a feedback controller to adjust the electrical motors voltage with forwarding speed and angular velocity as a result, the optimum brush design for the sweeping step is finalized. using a feedback controller to adjust the electrical motor voltage with forwarding speed and angular velocity as a result, the optimum brush design for the sweeping step is finalized.

Figure 2.8: Electrically powered brushing system

Figure 2.9: Sweeping system test on flat ground

### 2.2.6 Final Design - Comprehensive Control System for Optimized Sweeping

In the final iteration of the almond pickup system, significant improvements have been integrated into the sweeping section, effectively overcoming the challenges observed in the preceding prototypes. This advanced model now stands on par with commercial sweeping systems available on the market, both in terms of the sweeping rate and the minimal level of dust generation during the harvest. Two pivotal factors contribute to the optimized sweeping rate and dust control: the precise gap between the brushes and the ground, and the angular velocity of the brushes. To regulate the brush height, we have installed a height sensor for each sweeper unit, positioned strategically in front of each brush assembly. These sensors are interfaced with actuators that dynamically adjust the height based on real-time ground clearance data, ensuring the brushes maintain an optimal distance from the ground to prevent dust upheaval. In tandem with height control, the angular velocity of the brushes is critically managed to harmonize with the forward motion of the tractor. A well-calibrated balance between the tractor's speed and the rotational speed of the brushes is essential to ensure comprehensive coverage of the swept area. Each sweep of the brush is precisely timed and executed to touch the ground once, thereby minimizing the disturbance of the soil and the resultant dust emissions. This section delves into the mathematical modeling needed to establish a robust correlation between these two factors. The model aims to define the optimal conditions under which the brushes operate in synchrony with the tractor's movement, achieving a sweeping action that is both thorough and gentle. The model's parameters are fine-tuned to ensure that the brushes engage with the almonds effectively without agitating the soil unnecessarily, thus adhering to the overarching goal of the project to minimize dust generation.


Figure 2.10: Final prototype of the almond pickup system with integrated sweeping mechanism

### 2.2.7 Robotic Prototype - The Dawn of Autonomous Almond Harvesting

#### 2.2.7.1 Introducing a self-contained, electric platform marking a shift towards robotic harvesting.

Finally, I explored a significant advancement in agricultural technology: the robotic almond harvesting system. This innovative system embodies the principles of automation and energy efficiency. It operates as an electrically powered, self-sufficient unit, designed to function autonomously in agricultural fields. At its core is a robust electrical frame, which is named "Farm ng." This frame accommodates a generator, a battery, and a voltage regulator, ensuring a consistent 12-volt output.

This stable power supply is essential for efficiently operating key components like the sweeping brushes and the horizontal pickup brush motors, without any voltage fluctuations. A pivotal aspect of this system is the removal of the tractor from the harvesting process. This not only simplifies the design but also significantly reduces the carbon footprint associated with almond harvesting. The autonomous nature of this system addresses and improves upon the limitations of previous tractor-dependent models. The electric power allows for precise control over the brush speeds, leading to more efficient almond pickup, minimizing waste, and maximizing yield. Moreover, the self-contained design of this prototype paves the way for a future where fields can be harvested with little to no human intervention. This could lead to improvements in safety, cost-effectiveness, and the consistency of the operation. My research presents this innovation as a clear indication of the evolving direction of modern agriculture, focusing on creating sustainable, high-efficiency harvesting methods that align with the increasing demands of food production and environmental stewardship.


Figure 2.11: Farm-ng electrical frame


Figure 2.12: Robotic Prototype for future autonomous almond harvesting

# Chapter 3

# ENGINEERING AN OPTIMAL ALMOND SWEEPING MECHANISM

## 3.1 Introduction

Trunk shaker harvesting machines are a common tool used in the harvest of almonds in California. These machines function by vibrating the trees, causing the almond nuts to fall to the ground. Once the nuts have reached the desired moisture content, they are gathered into windrows using sweepers. The sweeping process begins by blowing the nuts between the tree lines and then sweeping the almonds toward the middle rows. After the sweeping operation, a pickup machine can then collect the nuts from the ground. One way to decrease the amount of dust generated during the harvest process is to design a more efficient sweeping system that has minimal interaction with the soil. By reducing the amount of soil disturbance during the sweeping process, it is possible to decrease the amount of dust generated, making the harvest process more efficient and less harmful to the environment.

### 3.1.1 Background

The issue of dust generated during the almond harvesting process has been a significant concern for the manufacturers of the equipment used in the process. To address this issue, several attempts have been made to modify the equipment to reduce the amount of dust produced. These efforts have primarily focused on trying to lower the dust after the pickup step. However, despite these attempts, the dust level generated during the almond harvest process remains high. Table 1.3 provides a summary of the modifications made by some of the commercial harvesting equipment manufacturers to reduce dust. One manufacturer, 'Exact Corporations', attempted to reduce dust by spraying water on it, but this approach resulted in additional problems, such as the need for maintenance to remove the mud generated in the container and slowing down the harvest process due to the need for refilling the water tank. Another manufacturer, "Flory Industries", tried to reduce dust by making the conveyor belt transfer almonds to the hopper longer, but this approach was not successful in significantly reducing the dust level. Jackrabbit Corporation designed a disk-based cleaning section to separate dust from almonds, but even this approach has its limitations. It would be more effective if the harvesting system was designed to generate less dust in the first place, rather than focusing on suppressing the dust that has already been generated. Despite the efforts made by various manufacturers, there remains a need to effectively reduce the dust level during the almond harvest process.

### 3.1.2 Related works

Previously reported agricultural-related research works in this area have been done mainly on header height control systems for Combine. In 2014, Yangmin Xie et al. designed a feedback controller for achieving robust stability and performance for Grain combine harvester header height control. An offline tracking system was used in their study to determine the shape of the ground before harvesting. In their study, they observed a large elevation change in a short distance due to the rapid changes in ground topology. To avoid causing equipment damage, they limited the maximum combined speed to 0.4 mph (0.64 km/h) using a controller [13]. Shuqi Shang (2022) presented an adaptive method for controlling headers' height. The height error of cutting stubble is about 2 cm, which meets the requirements of a 5–11 km/h harvesting speed in plain areas [14]. Yangmin Xie (2010) developed a state-feedback LQR controller for grain combine harvesters that allows adjustability according to ground shape [15]. A soybean harvester header-height adjustment system was developed by Chengqian Jin et al. in 2021. They designed it to eliminate the problems of improper harvesting and soil shoveling resulting from low-positioned soybean plants and inadequate header height control. The effect of soil compactness on the ground profile control accuracy of the header-height control system was one of the limitations of their study [16]. Xie et al. (2013) investigated the fundamental performance limitations of their header height control system for a grain combine harvester. In their study, the closed-loop performance was limited by the hydraulic actuator's time delay. For the system to have a low natural frequency, they had to redesign key parameters, such as suspension elements [17]. The grain Combine harvester header height tracking controller designed by Al Sawafi et al. (2021) used a fuzzy adaptive PID controller. When the fuzzy system is present, the PID control system changes its gain instantly to compensate. While the combine harvester was moving and tracking the change in the ground topology, the sensor, and fuzzy logic were read and recorded. Due to their nonlinear nature, fuzzy controllers are more difficult to set than proportional-integral-derivative controllers and the fuzzy control's inputs caused errors in their system [18]. Punit Tulpule et al. (2014) improved header height control performance in a Combine harvester by applying a sensitivity-based integrated robust optimal design methodology. The combination of their design and sequential methods resulted in a more robust and well-integrated system that can be controlled with less control power. Therefore, the vehicle's speed is increased, and operating costs are reduced [19]. For sugarcane harvester base-cutter control, Jun Zhang et al. (2022) used ground penetrating radar signals to automatically control the height of the base-cutter, they presented a method based on ground penetration radar (GPR). Using a knockdown roller mounted on a 1.6GHz GPR antenna, they measured the vertical distance between the ground and air-coupled GPR antenna. Due to limitations caused by a minimum error of ground layer detection of 1.76 cm, base-cutter height only varied by 1.46 cm [20]. A robust two-DOF controller for delayed LTI systems was introduced by Xie et al. (2013). During rapid changes in external signals, such as reference signals and/or disturbances, the system's feedback control loop is restricted, resulting in a reduced response capability. As a result, the delay term of the feedback controller was eliminated without affecting the H, norm of the objective functions [21]. One-rotor orchard inter-row analysis based on tines trajectory was designed by Lei XiaoHui et al. in 2019. An inter-row rake with one rotor was developed to improve orchard mechanization efficiency [22].

### 3.1.3 Objectives

This study aimed to design a height and speed controller for a newly designed almond sweeper and pickup system. We designed PID feedback controllers using SIMULINK and identified the system dynamics of the mechanism. A minimum amount of contact with the orchard floor was achieved by synchronizing brush rotational speed with the forward velocity of the harvester while adjusting the sweepers' heights to minimize dust generation by ensuring they only touch nuts, not dirt, debris, stones, or fruit.

## 3.2 Materials and Methods

### 3.2.1 Mathematical modeling for sweeping system

Figure 3.1 shows the prototype of the newly designed sweeper system. During the sweeping process (Figure 3.2), in the machine's operation, it moves along the Y-axis while the disc rotates in a counterclockwise direction. The negative direction of the X-axis is the location where the almonds are placed on the ground. As the disc rotates, the tines are utilized to sweep the nuts into a row. During the rotation of the disc from point 1 to point 2, the tines are in contact with the nuts, guiding them into a row. However, during the rotation from point 2 back to point 1, there is no contact between the tines and the ground.

Figure 3.1: Sweeping mechanism

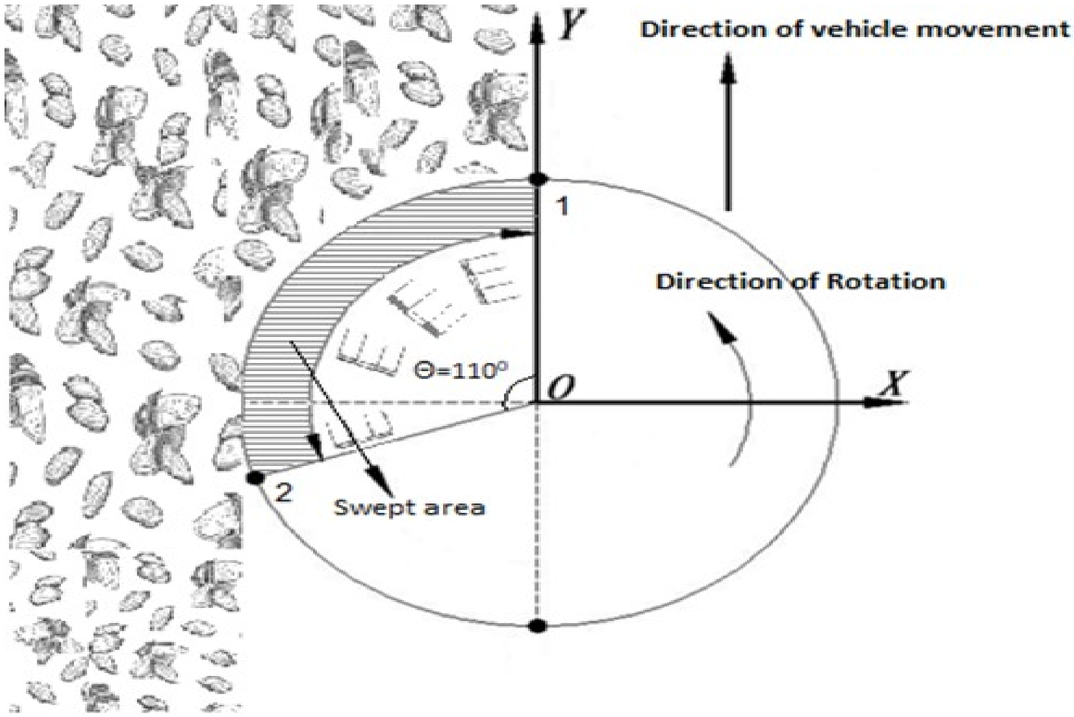


Figure 3.2: The stationary plane trajectory of the sweeper

The forward speed of the sweeper was set as $v$, the rotational speed was $\omega$, the rotational radius was r, the arm number was n, and the tine working width was L. In the plane trajectory of tines movement (Fig.3.3), points a and a' are the outermost positions of tines working on the first arm, points b and b' are the innermost positions of tines working on the first arm, points c and c' are the outermost positions of tines working on the second arm, point d and d' are the innermost positions of tines working on the second arm. The thick solid line area (aa'b'b) is the tines trajectory of the first arm, the thick dashed line area (cc'd'd) is the tines trajectory of the second arm, the miss raking area is the uncrossed area of the tines working, while the repeat raking area is two or more times crossed area of the tines working. Define miss raking rate as the ratio of miss raking area and working area in one cycle of disc rotation and repeat raking rate as the ratio of repeat raking area and working area in one cycle of disc rotation.

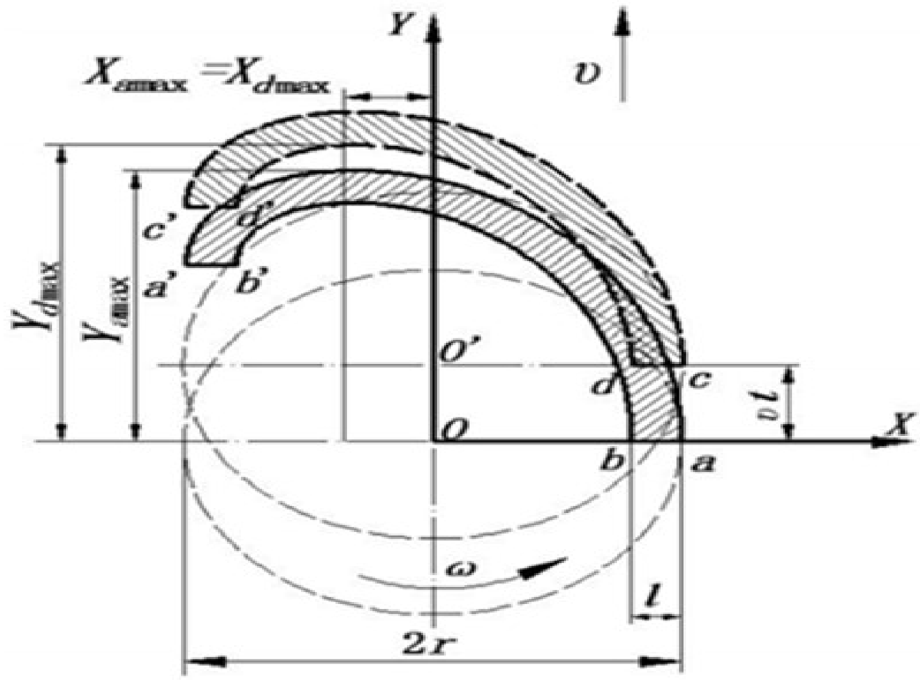


Figure 3.3: The Plane trajectory of tines movement

The movement equation of point a is:

$$\begin{aligned} X_a &= r\cos(\omega t) \\ Y_a &= r\sin(\omega t) + vt \end{aligned} \tag{3.1}$$

where $X_a$ is the value of point a on the X axis, $Y_a$ is the value of point a on the Y axis, and $t$ is working time. The movement equation of point d is:

$$\begin{aligned} X_d &= (r-l)\cos\left(\omega\ t - \frac{2\pi}{n}\right) \\ Y_d &= (r-l)\ \sin(\omega t - 2\pi/n) + vt \end{aligned} \tag{3.2}$$

where $X_d$ is the value of point d on the X axis, and $Y_d$ is the value of point d on the Y axis. The maximum values of point a and point d on the Y axis can be found by setting derivatives $Y_a$ and $Y_d$ in equations (3.1) and (3.2) to zero. We obtain:

$$Y_{amax} = \frac{v}{\omega}\arccos\left(-\frac{v}{\omega\ r}\right) + r\sin\left[\arccos\left(-\frac{v}{\omega\ r}\right)\right] \tag{3.3}$$

$$Y_{dmax} = v\left[\frac{2\pi}{\omega\ n} + \frac{1}{\omega}\arccos\left(-\frac{v}{\omega\,(r-l)}\right)\right] + (r-l)\sin\left[\arccos\left(-\frac{v}{\omega\,(r-l)}\right)\right] \tag{3.4}$$

where $Y_{dmax}$ is the max value of point a on the Y axis, $Y_{dmax}$ is the max value of point d on the Y axis. In one cycle of brush rotation, if $Y_{amax} < Y_{dmax}$, there are two intersections between point a trajectory and point d trajectory, and the blank area between two intersections is miss raking zone. If $Y_{amax} = Y_{dmax}$, only one tangent point between point a trajectory and point d trajectory, and $X_{amax} = X_{dmax}$ at this moment, and the repeat raking zone is least, this is the optimal working state. If $Y_{amax} > Y_{dmax}$, there would be a larger repeat raking zone, a faster movement speed, and a lower disc rotational speed that can lead to improved brush performance. The ideal working condition for the brush is achieved when there is no gap or minimal overlap between the adjacent working areas of the tines. This ensures that all the area in front of the brush is effectively swept and that the tines are functioning optimally. Therefore, this means $Y_{amax} - Y_{dmax} \geq 0$. Based on detail parameters, getting:

$$\begin{aligned}&\sqrt{1-\frac{v^2}{\omega^2 r^2}}-\sqrt{\left(1-\frac{l}{r}\right)^2-\frac{v^2}{\omega^2 r^2}}\\&+\frac{v}{\omega\ r}\left[\arccos\frac{v}{\omega\,(r-l)}-\arccos\frac{v}{\omega\ r}\right]-\frac{2\pi v}{n\omega r}\geq 0\end{aligned} \tag{3.5}$$

The Equation (3.5) represents the optimal kinematic model for a one-rotor horizontal brush. In order for the brush to effectively sweep all the area in front of it, this equation should equal zero. This indicates that the brush is executing the proper motion and achieving complete coverage of the area in front of it.

### 3.2.2 Sweeper angular velocity controller design

The feed-forward reference adjustment for our control system is a critical component, as it helps to ensure accurate and efficient performance. The adjustment is based on a mathematical relationship between the forward speed and angular velocity of the brushes, which is described in Equation (3.5). Using the data obtained from the forward speed magnetic sensor, we can determine the precise angular velocity required for the brushes to operate effectively. In other words, the feed-forward reference adjustment allows us to adjust the speed and movement of the brushes based on the forward velocity of the harvester, which is a crucial factor in determining the performance of the system. The combination of this reference adjustment with the data from the magnetic sensor ensures that the brushes operate with optimal speed and efficiency, contributing to the overall success of our control system.

### 3.2.3 Sweeper motor system identification

The brushes in question are equipped with a Zipo electric motor, identified by the model number ATP50. This motor is responsible for powering the brush, and its output torque has been boosted using chains and sprockets, which connect the motor shaft to the brush shaft. The electrical motors used in this study were analyzed and their dynamics were determined through experimentation and the use of the MATLAB System Identification package. Unfortunately, the transfer functions for these motors were not readily available, so an experimental approach was taken to understand the electrical motors and brush dynamics. To accurately measure the performance of the sweeping system, two different instruments were employed. The first was a tachometer, which was used to determine the forward speed of the system. Additionally, a spindle speed meter sensor was used to measure the rotational velocity of the sweeping brush. The sweeping motor had a limited maximum angular velocity of 65 RPM, which was a key factor in determining the maximum forward speed. According to the results of Equation (3.5), this maximum forward speed was limited to 10 m/s. To further analyze the system, a graph was created showing the relationship between brush angular velocity and motor input voltage, as depicted in Figure3.4 To gain a deeper understanding of the system's dynamics, the MATLAB System Identification Toolbox was used to conduct a detailed analysis.

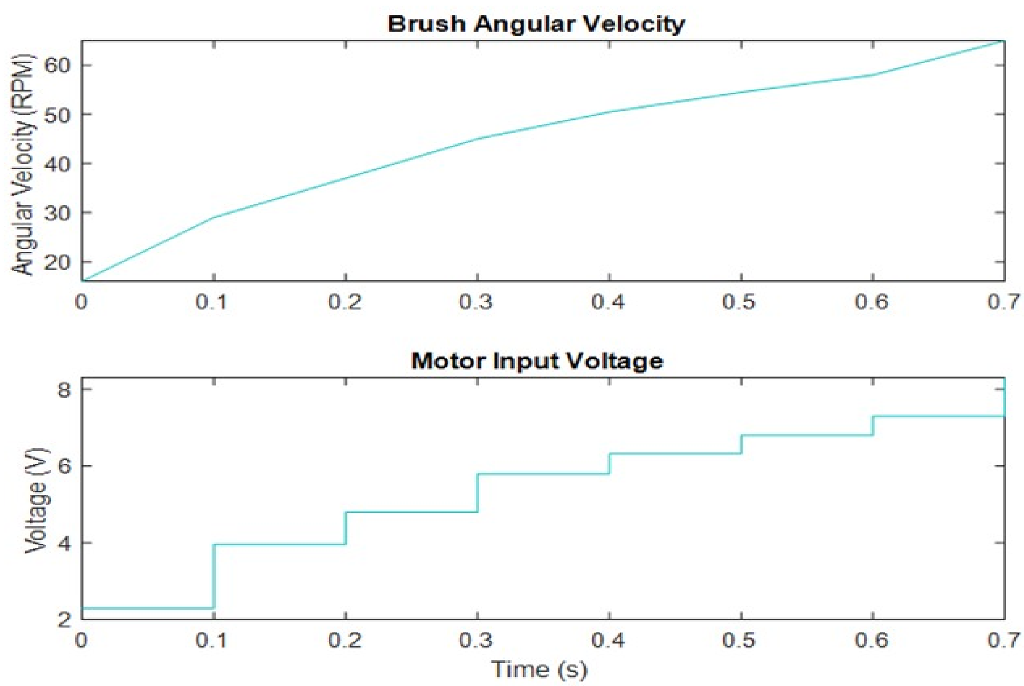


Figure 3.4: Brush angular velocity and motor input voltage

The motor and brush transfer function is as follows:

$$B_s(s) = \frac{\theta}{V} = \frac{8.7208}{0.0475\ s^2 + 0.1173\ s + 1} \tag{3.6}$$

### 3.2.4 Angular velocity control system

The block diagram in Figure3.5 served as the basis for the construction of a PID(Proportional Integral Derivative) controller for the dynamic system. By studying the block diagram, it was possible to design and implement a PID controller that would effectively control the behavior of the system. This type of controller is commonly used in a variety of applications and is well-suited to this particular dynamic system due to its ability to accurately respond to changes in system behavior and maintain control over the system. The implementation of the PID controller in accordance with the block diagram in Figure3.5 has allowed for precise control over the dynamic system and has ensured that the system operates in a stable and efficient manner.

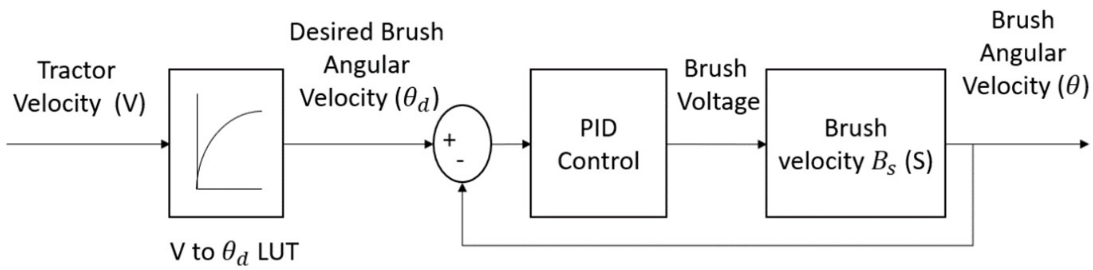


Figure 3.5: Control system block diagram for front brush angular speed regulation

The diagram represents the working principle of our control system, which is designed to regulate brush angular velocity in an almond harvesting system. The system starts with a feed-forward section, which tunes the brush angular velocity based on the forward speed of the vehicle. The forward speed is manually input into the system, and the brush angular velocity is determined based on this input, which is then fed back into the feedback system for regulation. A simulation was performed using a function for vehicle forward speed as the input to the control system. This simulation allowed us to determine the desired versus measured omega (brush angular velocity) and the necessary voltage for the motor to apply the desired angular velocity. The results of the simulation are shown in Figure3.6, which highlights the performance of the control system and its ability to accurately regulate brush angular velocity. In summary, the diagram illustrates the functioning of a control system that is designed to regulate brush angular velocity in an almond harvesting system. The feed-forward section tunes the brush angular velocity based on the vehicle's forward speed, and the simulation results show the accuracy and efficiency of the system in regulating brush angular velocity.

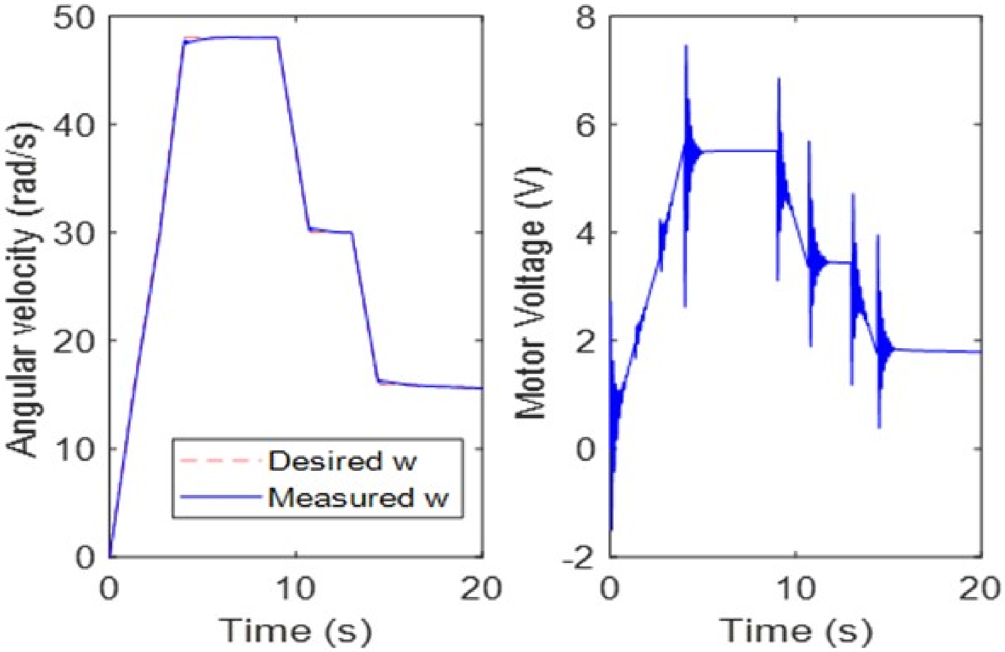


Figure 3.6: Front brush tracking control response with PID controller

Figure3.6 demonstrates the performance of the control system in regulating brush angular velocity based on the forward speed of the vehicle. As the forward speed increases, the angular velocity also increases, following the trend defined in the first section of the omega-time curve. This relationship is confirmed by Equation (3.5), which demonstrates the correlation between forward speed and brush angular speed. In the second section of the curve, we see a constant forward speed that is maintained by a fixed angular velocity. The vehicle moves forward at two decelerations and two constant speeds. Figure3.7 shows that the desired omega tracks the measured omega with good accuracy. This indicates that the control system is functioning effectively in regulating brush angular velocity based on the forward speed of the vehicle. The settling time, which is the time it takes for the system to reach its final steady-state value, was found to be 0.57 seconds, which is a small value and indicates that the control system responds quickly to changes in the forward speed. Additionally, the overshoot, which is the maximum deviation from the final steady-state value, is also minimal, further demonstrating the effectiveness of the control system.

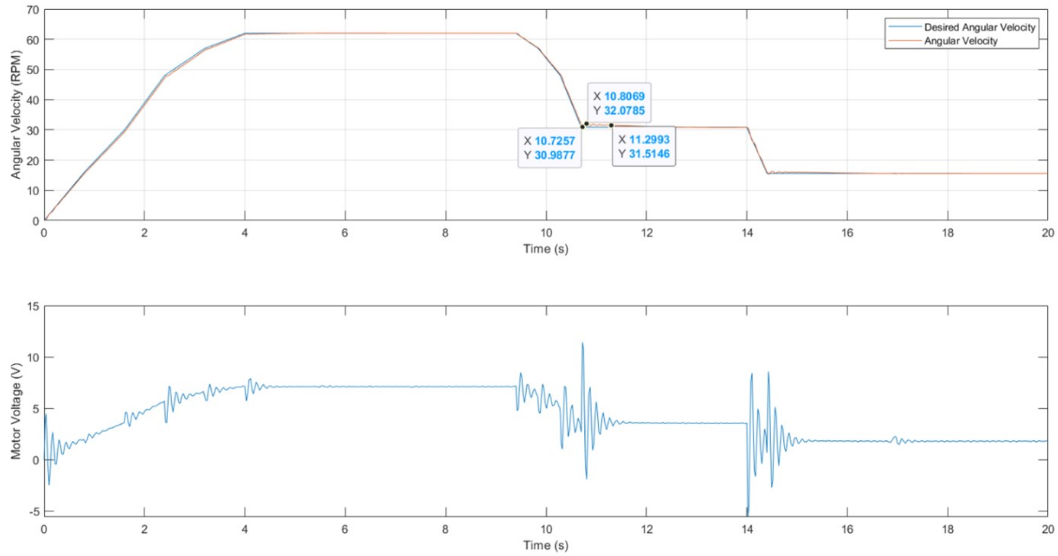


Figure 3.7: Front brush tracking control response with PID controller with overshoot and settling time

### 3.2.5 Linear actuator height controller design

For each sweeper, we must use a closed-loop control system to specify the brush height so that the gap with the ground is 0.5 inches. This 0.5-inch distance between the brush edge and floor is less than the thickness of one almond with shell on the orchard floor, which will help just sweep the fruit and minimize brush/orchard floor contact to minimize dust generation.

### 3.2.6 Linear actuator system identification

The height of each brush is controlled through the use of an actuator. The specific actuators utilized in this study are manufactured by Progressive Automation Co. and are identified by the part number PA-04-6-100. These actuators have a 12 VDC power supply, a 6-inch stroke, and a maximum weight capacity of 100 lbs. To ensure precise control over the length of the actuators, feedback from two optical distance sensors is employed. These sensors are mounted on each sweeper and provide real-time data to inform the control system and make necessary adjustments to the actuator length. To control the height of the brushes, an actuator is utilized. The actuators used in this study come from Progressive Automation Co. and have a part number of PA-04-6-100. These actuators are powered by a 12 VDC power supply and have a 6-inch stroke length and a weight capacity of 100 lbs. To maintain precise control over the length of the actuators, two optical distance sensors are utilized to provide real-time feedback to the control system. These sensors are mounted on each sweeper and allow for accurate monitoring of the actuator length, allowing for prompt adjustments to be made as necessary. To determine the average speed of the actuator's motion, an experimental method was used where the weight was lifted down at a faster rate than it was lifted up. However, this approach introduced some inaccuracies in the calculations, which could be corrected through compensation in the control simulation to ensure that the lifting speed is similar in both the upward and downward motions. The dynamic behavior of the actuator/brush height system was also analyzed using the MATLAB System Identification Package, providing a deeper understanding of the system's performance. The transfer function of the height actuator:

$$A_s(s) = \frac{L}{V} = \frac{0.0078156}{0.21617\ s^2 + 0.1951\ s + 1} \tag{3.7}$$

### 3.2.7 Linear actuator control system

The adjustment compensatory for the motor's lift up/down speeds:

$$P + I\left(\frac{1}{s}\right) + D\left(\frac{N}{1 + N\frac{1}{s}}\right) \tag{3.8}$$

The compensator uses the following parameters:

$$\begin{aligned} P &= 20; \\ I &= 0.05; \\ D &= 10; \\ N &= 10 \end{aligned} \tag{3.9}$$

Where N is the number of the filter coefficients. When designing the control system for a sweeping system with two brushes, it is essential to take into account the unique requirements of each brush. This is due to the fact that in a real-world application, the controller must accurately position different tracks in front of each brush, ensuring that no fruit is missed and that the brush is not damaged in the process. To achieve this goal, it is necessary to create two separate control block diagrams. These diagrams will outline the specific requirements and parameters for each brush, allowing for precise and effective control over the sweeping system. In this way, we can ensure that the sweeping system operates efficiently and effectively, minimizing any damage to the brushes and maximizing the collection of fruit.

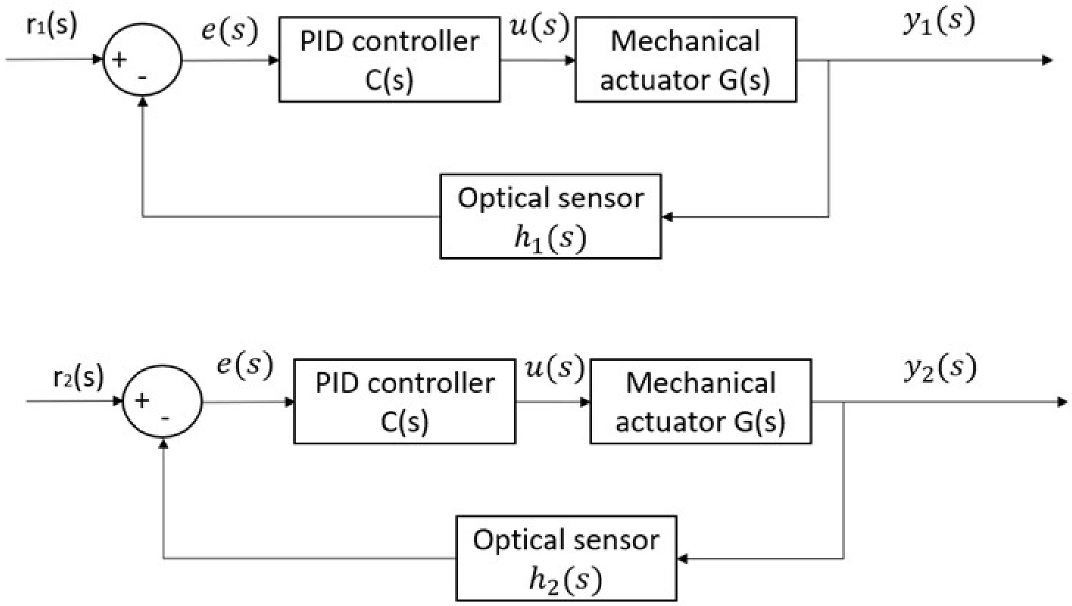


Figure 3.8: Control system block diagram for front brushes height

As a semi-realistic track with a period of 35 seconds, we have established a sinusoidal wave to symbolize the height controller located in front of both brush units. The height controller plays a crucial role in ensuring that the brushes maintain a consistent height as they travel along the track, which is essential for creating a smooth and even surface. The use of a sinusoidal wave to represent the height controller allows us to accurately simulate the changing heights of the brushes in a controlled and predictable manner. This helps us to thoroughly test the performance of the brushes and ensure that they will work effectively in real-world conditions. Overall, the sinusoidal wave serves as an effective tool for modeling and evaluating the height control system of the brushes.

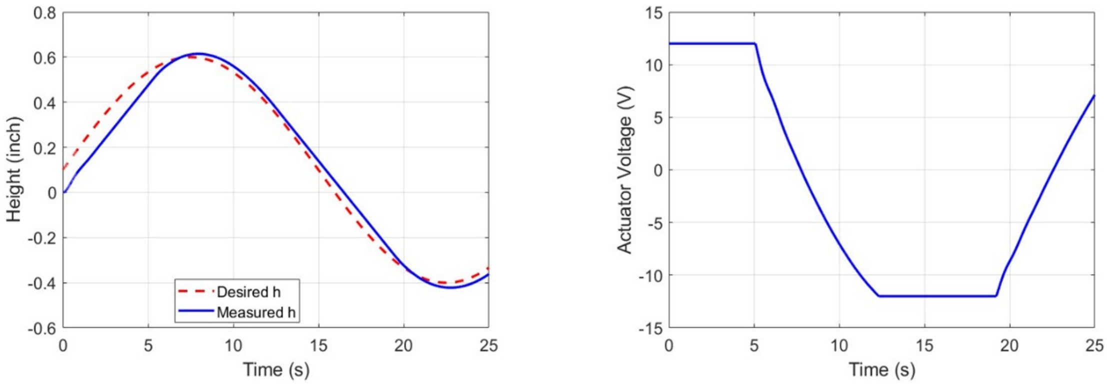


Figure 3.9: Front brush height control response with PID controller

The graph in Figure3.9 provides a visual representation of the response of the front brush height control, as well as the voltage that is applied to it. As the actuator voltage graph indicates, the voltage remains constant at 12 volts from time 0 to 5 seconds and then changes to -12 volts from time 12 to 18 seconds. It's important to note that our actuators have a maximum capacity of 12 volts, so they cannot exceed their rated voltage when more power is needed. In Figure3.8, we can observe the impact of saturation on the actuator response time, which results in a decrease in the lift up/down speed during the period of saturation. The slow response time of the actuator is due to the limitations imposed by saturation, which negatively affects the overall performance of the system. To overcome this issue, engineers and designers need to consider ways to prevent saturation from occurring, so that the actuators can operate at their maximum potential, providing fast and reliable control over the front brush height.

## 3.3 Performance Results

Our lab test was thoroughly designed to mimic real orchard conditions and we made sure to use soil, dried leaves, debris, etc. that were representative of an actual almond orchard. We used low-dust harvester results as a baseline to compare our results against and were able to demonstrate that our newly designed almond sweeper and pickup system generated significantly less dust (measured as PM2.5 and PM10) compared to the existing low-dust harvester being used in the field [23]. We recorded these results and compared them to data from tests performed in real orchards. Table 3.1 showcases the comparison between our lab test results and the real orchard tests. Despite the promising results from our lab test, we understand that it is still important to perform tests in real orchards to get more data and optimize our design further. Hence, we plan to conduct tests during the upcoming harvest season to validate our design under real orchard conditions.

Table 3.1: Dust generation for the lab test versus field test results

| **Average $PM_{2.5}$ (Lab test)** | **Average $PM_{2.5}$ (Field test)** | **Improvement** | **Average $PM_{10}$ (Lab test)** | **Average $PM_{10}$ (Field test)** | **Improvement** |
|---|---|---|---|---|---|
| 44 $\mu g/m^3$ | 700 $\mu g/m^3$ | %94 | 80 $\mu g/m^3$ | 1015 $\mu g/m^3$ | %92 |

## 3.4 Conclusion

The primary objective of this study is to develop a control system for the sweepers of an almond harvester that can maintain optimum contact between the brush, orchard floor, and fruit. This is done to reduce the amount of dust generated during the harvest process, which is a major concern during the California harvest season. Dust can cause respiratory problems for the workers involved in the harvest, as well as cause damage to the quality of the fruit. In order to make our control system compatible with the existing system, two feedback systems were designed and tested. Although there were a few limitations in our system, including the limited rated voltage of the actuators that resulted in delayed response time and the limited ability of the electrical motors to increase Omega above 65 rpm, the controllers still performed well enough for our harvester mechanism. Despite these limitations, our study aims to address a critical problem in the almond harvest industry and provide a solution that can be implemented to reduce dust generation during the harvest process.

# Chapter 4

# PREDICTIVE NEURAL NETWORK MODELING FOR ALMOND HARVEST DUST CONTROL

## 4.1 Introduction

### 4.1.1 Background of the Problem

Almond harvesting has traditionally been a dusty affair due to the nature of the operations involved. The conventional methods employed by harvesters like Flory [24], Weiss McNair [25], and Jack Rabbit [26], amongst others, have been known to produce a significant amount of particulate matter emissions during the harvesting process. Specifically, emissions from conventional harvesters were compared to those from low-dust harvesters like Flory 850, Exact E3800, Weiss-McNair 9800, and Jack Rabbit in orchards located in Fresno County, demonstrating that the low-dust harvesters produced fewer emissions. A notable challenge within the almond harvesting industry in California has been the lack of an available particulate matter (PM) PM2.5 emission factor for the operations. This gap has posed challenges for particulate matter regulations and emissions inventory within the state. Low-dust harvesters have been seen as a viable strategy to reduce PM emissions and help achieve the state's PM2.5 attainment targets [27, 28].

### 4.1.2 Importance of Predicting PM2.5

The control and reduction of particulate matter emissions are crucial for both environmental and human health. Particularly, PM2.5 (particles with a diameter of 2.5 micrometers or smaller) is of concern as these particles can be inhaled into the lungs and even enter the bloodstream. Predicting PM2.5 emissions from almond harvesting operations can provide crucial insights for regulatory compliance, operational adjustments, and the development of low-emission harvesting technologies. By accurately predicting PM2.5 emissions, stakeholders can make informed decisions to mitigate environmental impacts, adhere to regulatory standards, and improve the overall sustainability of almond harvesting operations.

### 4.1.3 Objectives

The primary objective of this chapter is to develop a predictive model utilizing neural networks to estimate PM2.5 emissions based on various operational parameters of a newly designed almond harvester. Through rigorous data collection, preprocessing, and model development, this chapter aims to provide a robust predictive model that can be used by stakeholders to assess and mitigate PM2.5 emissions from almond harvesting operations. Additionally, this chapter will explore the potential of leveraging such a model in real-time monitoring and control of almond harvesting operations to minimize particulate matter emissions. In the subsequent sections, we will delve deeper into the methodological approach, data collection, and preprocessing, model development and evaluation, and the practical implications of the predictive model in addressing the particulate matter emission challenges in almond harvesting.

### 4.1.4 Literature Review

The prediction of emissions in agricultural settings using neural network models has attracted research interest over the years. Numerous studies have aimed at modeling different greenhouse gases using such models. This section provides an overview of existing literature on the use of neural network models in predicting emissions in agriculture, particularly focusing on the relevance to the prediction of PM2.5 emissions during almond harvesting.

### 4.1.5 Emission Prediction in Agriculture

Several studies have been conducted to predict emissions from agricultural activities using neural networks. For instance, a study aimed to model CO2 flux from soil to atmosphere in greenhouse conditions using multiple linear regression, artificial neural networks (ANN), and deep learning neural networks (DLNN), with parameters like crop species, soil temperature, soil moisture content, photosynthetic active radiation (PAR), and soil oxygen exchange as input parameters for predicting CO2 flux [29]. Another study employed a Feedforward Neural Network constructed using the Sequential Neural Network in Keras to predict CO2 and CH4 emissions for Onion crops from open farms and polyhouses [30]. Additionally, a novel methodology based on neural networks was discussed to determine agriculture emission model simulations, focusing on methane and nitrous oxide emissions, thereby enabling a more structured approach to emission prediction [31] .

### 4.1.6 Neural Network Models for Agricultural Emissions

Various studies have explored different configurations of neural network models to optimize the prediction of agricultural emissions. A study examined different combinations of layers and neurons to identify the best regression ANN models for predicting agricultural methane and CO2 emissions, using training SSE, Testing SSE, and RMSE as output measurement methods to choose the best model9.

Another study applied artificial neural networks to predict output energy and greenhouse gas (GHG) emissions in potato production in Iran, demonstrating the versatility of neural network models in predicting different types of emissions across various agricultural products and regions [32].

### 4.1.7 Previous work on dust prediction and related problems

Research and practical work have been conducted to understand and manage dust emissions in various industries, including agriculture. Notable work includes:

- Studies have highlighted dust generation as a significant concern in agricultural settings, where operations like harvesting, tillage, and other field activities contribute to airborne particulate matter [33].
- Development and implementation of dust monitoring and control technologies to mitigate the environmental and health impacts of dust emissions from agricultural operations [34].
- Proposition of methods to model and predict dust emissions based on factors like soil characteristics, weather conditions, and operational parameters, aiding in proactive management of dust emissions [35].
- Exploration of remote sensing technologies for monitoring soil erosion and dust generation in agricultural fields, providing valuable data for understanding and controlling dust emissions [28].

### 4.1.8 Advancements in Neural Network applications for environmental engineering problems

The application of Artificial Neural Networks (ANNs) has been rapidly advancing in the field of environmental engineering due to the capability of ANNs to handle complex, nonlinear relationships inherent in environmental data. Notable advancements include:

- Significant innovations and developments in the application of ANN as a tool of Artificial Intelligence over the last two decades [36].
- Applications of Neural Networks in various facets of Environmental Engineering, providing solutions to complex environmental engineering problems such as solid waste disposal, public health impacts, recycling strategies, and pollution control [37].
- ANNs demonstrate a high level of competency in solving complex engineering problems beyond the computational capability of classical mathematics and traditional procedures, addressing issues like pollution control and waste management among others [38].

### 4.1.9 Relevance to PM2.5 Prediction in Almond Harvesting

The literature reveals the robustness and flexibility of neural network models in predicting different types of emissions across a range of agricultural activities. While there's a scarcity of literature specifically focusing on PM2.5 emissions during almond harvesting, the discussed studies provide a solid foundation and justification for the application of neural network models in this domain. The adaptable nature of neural network models, as demonstrated in the literature, provides a promising avenue for developing accurate and reliable models for predicting PM2.5 emissions in almond harvesting operations.

## 4.2 Data Collection and Preprocessing

### 4.2.1 Description of the Dataset

The data set utilized for this study is derived from meticulous field observations and measurements taken during the almond harvesting season. The data, organized in an Excel spreadsheet, encapsulates various parameters considered influential in the emanation of PM2.5 emissions. The data set comprises five columns representing:

- Horizontal Brush Speed (rpm): The rotational speed of the horizontal brush.
- Angular Velocity of Vertical Brushes (rpm): The rotational speed of the two vertical brushes employed as sweepers.
- Forward Speed (m/s): The forward speed of the harvester.
- Measured PM2.5: Recorded PM2.5 emissions during harvesting.
- Measured PM10: Recorded PM10 emissions during harvesting.

One of the pivotal inquiries of this study is to discern the correlation between PM2.5 and PM10 emissions, scrutinizing whether one can serve as a proxy for the other, thereby simplifying the neural network model.

### 4.2.2 Outlier Detection and Removal

Given the propensity of outliers to skew the model learning process adversely, a rigorous outlier detection and removal process was undertaken. The Interquartile Range (IQR) method was employed to identify and expunge outliers from data set [39]. Figure4.1 illustrates the outliers before and after removal.

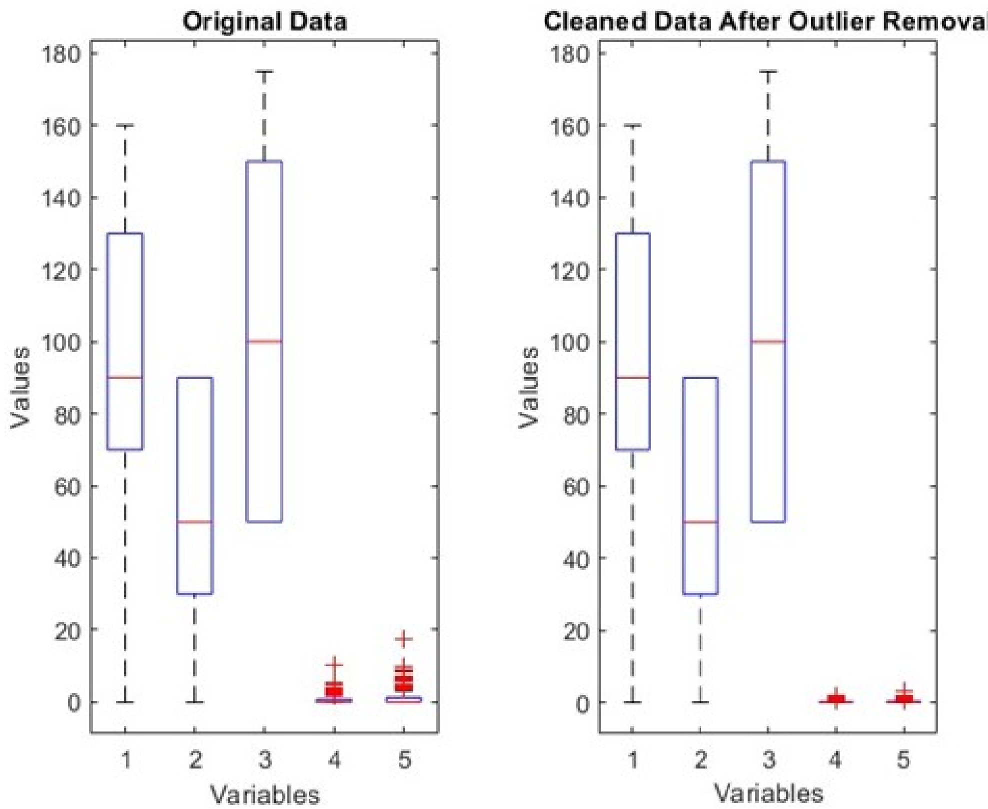


Figure 4.1: Outlier detection and removal

### 4.2.3 Data Scaling and Normalization

To ensure a standardized scale promoting an efficient learning process, the data set underwent scaling and normalization. The Z-score normalization method was applied to the first three columns of the data set, representing the input features for the neural network model [40].

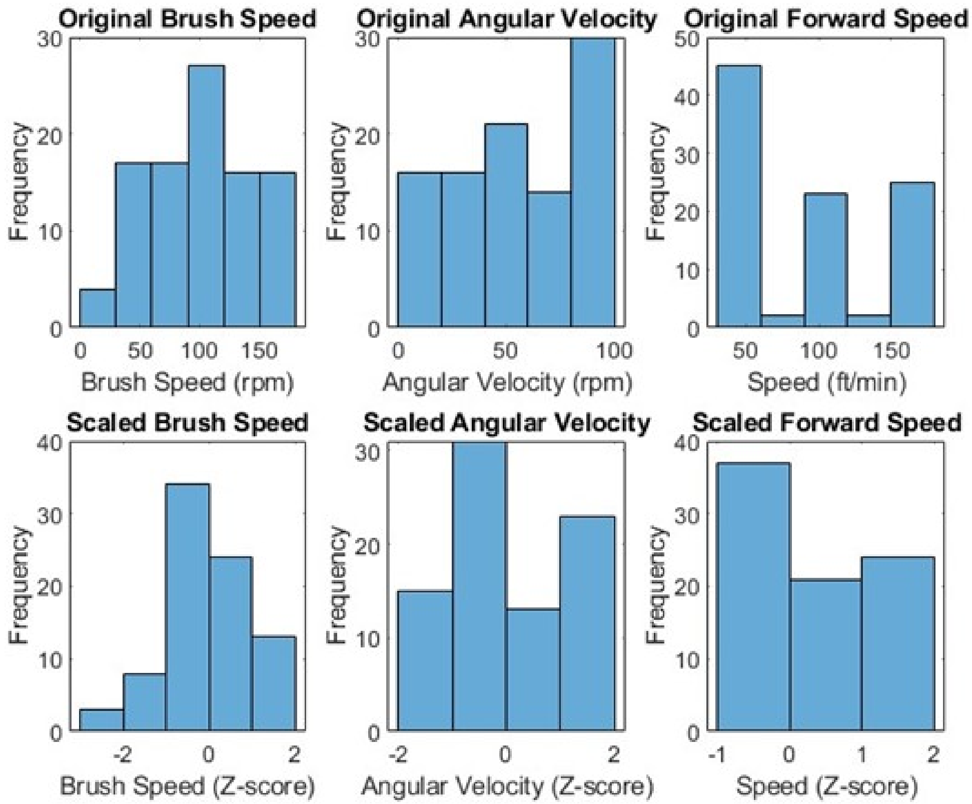


Figure 4.2: Data before and after scaling

These preprocessing steps were crucial in ensuring a clean, standardized data set, paving the way for the subsequent development of a robust neural network model to predict PM2.5 emissions during almond harvesting.

## 4.3 Exploratory Data Analysis

### 4.3.1 Correlation Analysis between PM2.5 and PM10

One of the initial steps in the data analysis process was to discern the relationship between PM2.5 and PM10 emissions. As documented in the literature, a strong correlation between these two particulate matter sizes is often witnessed due to their common sources and similar dispersion behaviors [41]. The correlation coefficient obtained was 0.99, indicating a very strong linear relationship between PM2.5 and PM10 emissions. This high degree of correlation suggests that PM2.5 emissions could potentially be employed as a proxy for PM10 emissions, thus simplifying the modeling process. Figure 4.3 elucidates the scatter plot illustrating the strong correlation between PM2.5 and PM10. PM2.5 PM10

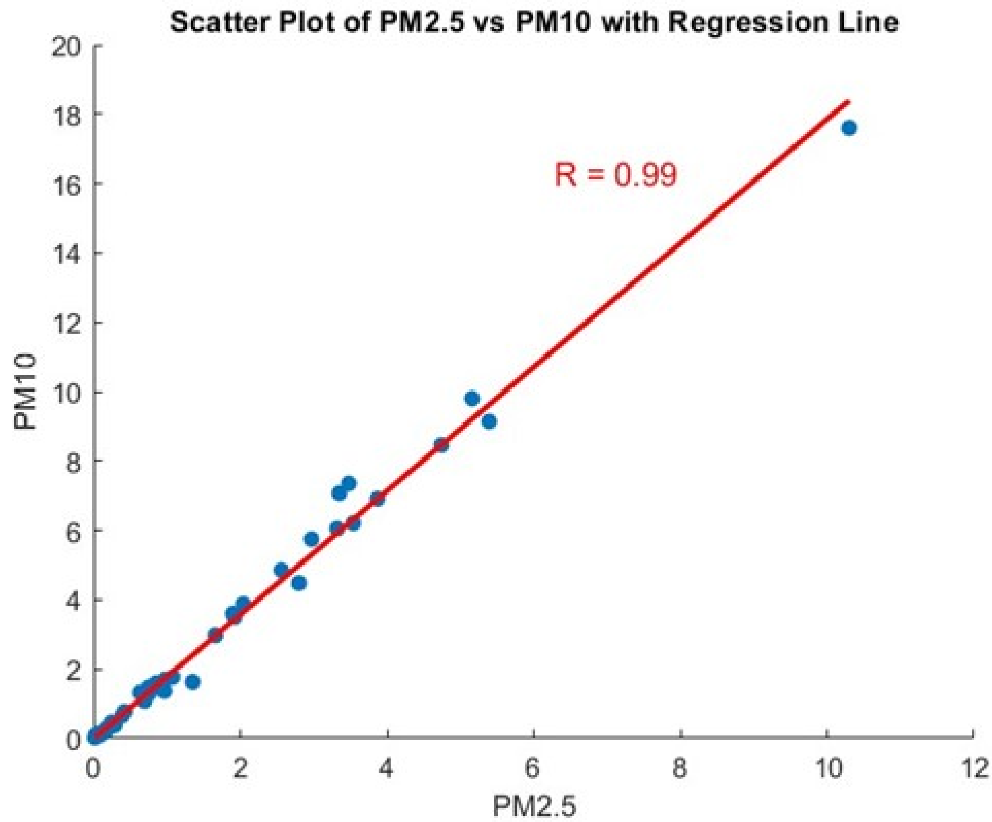


Figure 4.3: Scatter plot illustrating the correlation between PM2.5 and PM10 emissions(mg/m3)

### 4.3.2 Other Possible Analyses to Understand the Data Better

Understanding the data thoroughly is paramount to developing a robust predictive model. Besides the correlation analysis, several other exploratory data analysis (EDA) techniques were employed to glean insights from the data and to discern the relationships between the input features and the target variable (PM2.5). Some of these analyses include:

### 4.3.3 Descriptive Statistics

Descriptive statistics provide a summary of the central tendency, dispersion, and shape of the data set's distribution. Measures such as mean, median, standard deviation, skewness, and kurtosis are instrumental in understanding the data set's underlying structure [42].

### 4.3.4 Histogram Analysis:

Histograms are employed to visualize the distribution of the data. Figure4.4 shows the distribution of PM2.5 emissions, which is pivotal in understanding the skewness and kurtosis of the data.

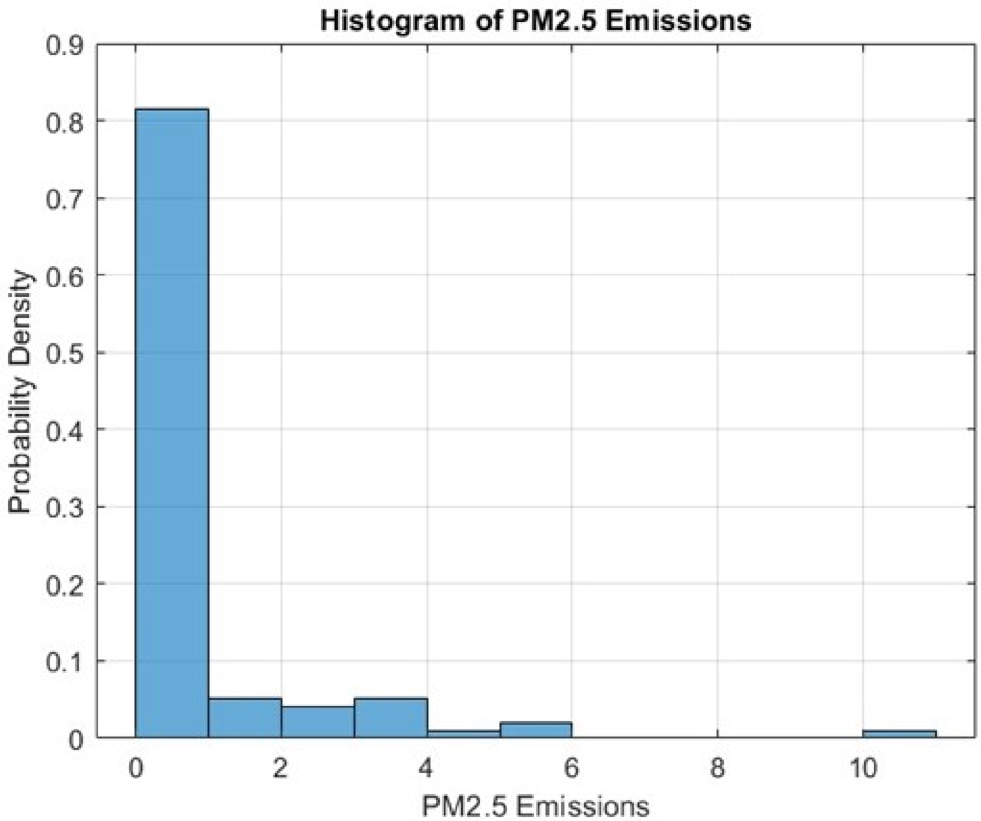


Figure 4.4: Histogram illustrating the distribution of PM2.5 emissions.

### 4.3.5 Boxplot Analysis:

Boxplots provide a visual summary of the minimum, first quartile (Q1), median, third quartile (Q3), and maximum of the dataset. It is also instrumental in identifying outliers post-cleansing.

### 4.3.6 Pairwise Correlation of All Variables:

Analyzing the correlation between all variables in the dataset helps in understanding the relationships and potential multicollinearity, which could affect the performance of the neural network model.

### 4.3.7 Heatmap of Correlations:

A heatmap provides a color-coded representation of the correlation matrix, assisting in visually identifying strong correlations between variables. Figure4.5 displays a heatmap of the correlations between all variables in the dataset.

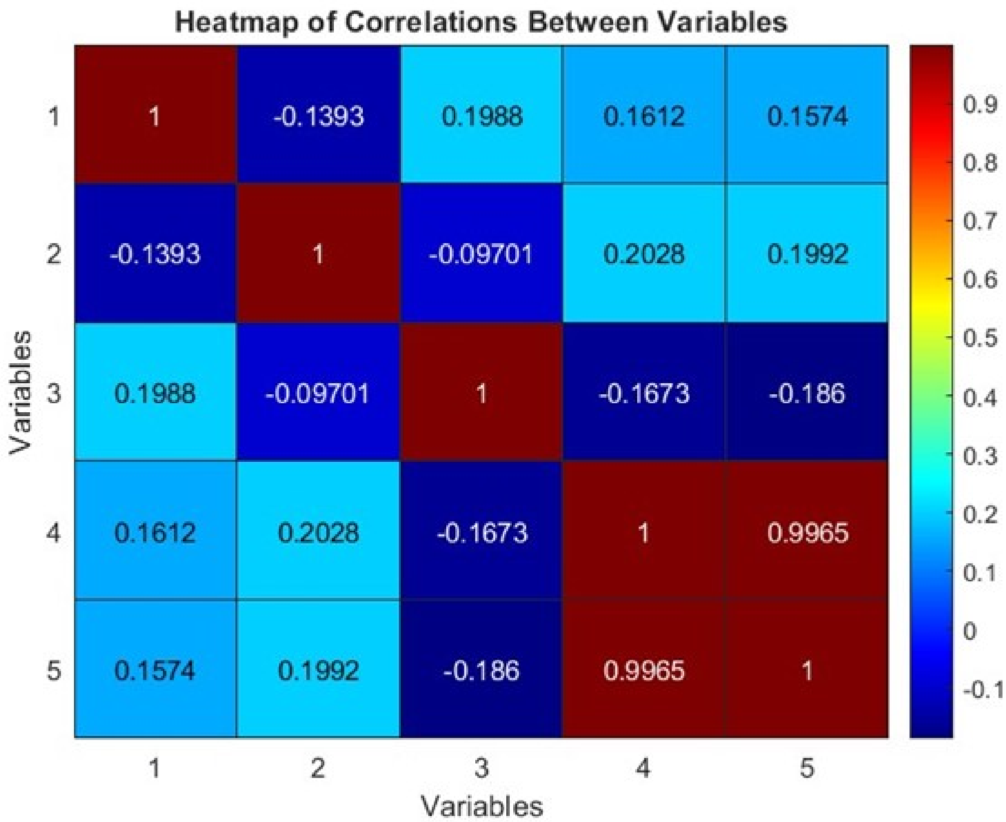


Figure 4.5: Heatmap illustrating the correlations between all variables in the dataset

These analyses were instrumental in understanding the underlying structure of the dataset, thereby informing the construction and training of the neural network model.

## 4.4 Neural Network Design

### 4.4.1 Choice of Neural Network Architecture

In addressing the problem of predicting PM2.5 emissions during almond harvesting based on the given input parameters, a neural network model was chosen for its ability to capture complex relationships between variables. Specifically, a feed-forward neural network (FNN) was selected due to its simplicity and efficacy in handling regression tasks [43]. The architecture of the neural network comprises an input layer, two hidden layers, and an output layer. The choice of two hidden layers was made to provide the model with enough capacity to learn from the data while avoiding overfitting. Each hidden layer contains three neurons, determined empirically to provide a good trade-off between model complexity and performance.

- Input Layer: The input layer consists of three neurons corresponding to the three input features: Horizontal Brush Speed, Angular Velocity of Vertical Brushes, and Forward Speed.

- Hidden Layers: The first hidden layer also comprises three neurons, allowing for the extraction and learning of features from the input data. The second hidden layer, also with three neurons, helps in further refining the learned features and passing them onto the output layer.

- Output Layer: The output layer contains a single neuron that outputs the predicted PM2.5 emission value.

### 4.4.2 Choice of Activation Functions, Loss Function, and Optimization Algorithm

- Activation Functions: The activation function in the hidden layers is the hyperbolic tangent (tanh) function. The tanh function was selected due to its ability to handle vanishing gradient problems better than the sigmoid function, and its capability to model both positive and negative relationships between variables2.

- Loss Function: The loss function chosen for this model is the Mean Squared Error (MSE) loss function. MSE is commonly used in regression problems for its ability to penalize larger errors more than smaller ones, thus driving the model to learn more accurate predictions3.

- Optimization Algorithm: The Adam optimization algorithm was employed for its efficiency in practice and little memory requirements4. Adam also adjusts the learning rate during training, which can lead to quicker convergence. The following diagram provides a visual representation of the neural network architecture.

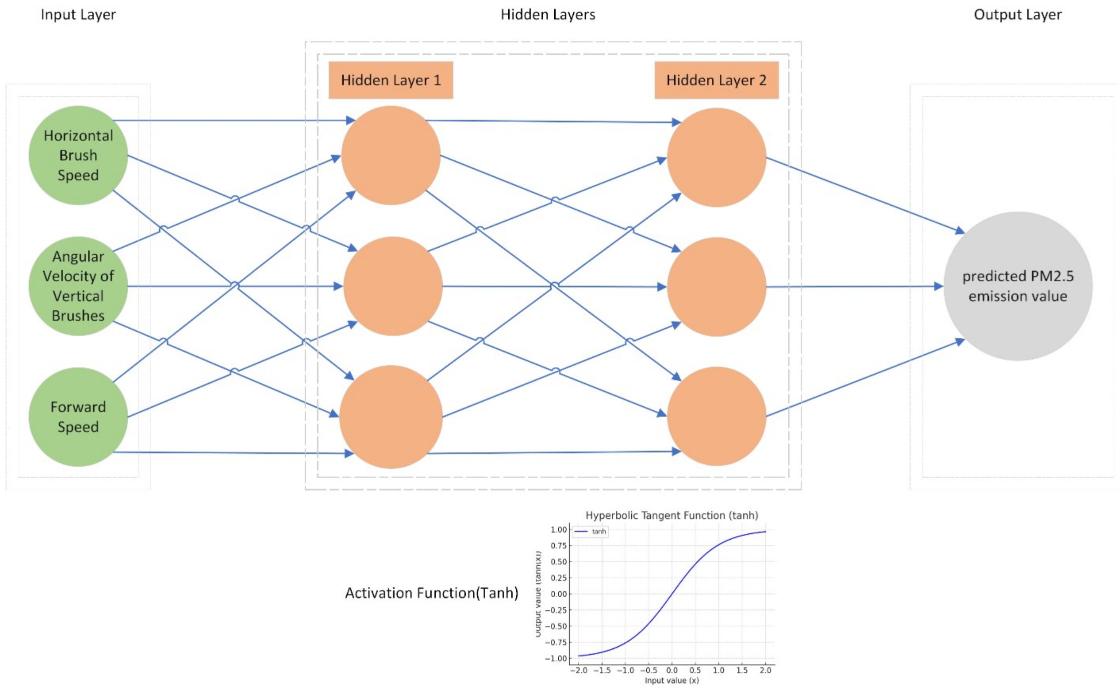


Figure 4.6: Diagram illustrating the architecture of the neural network model

The configurations were chosen based on a combination of empirical testing and theoretical justification, aligning with common practices in the field of machine learning.

### 4.4.3 Model Training and Validation

The process of training and validating the model is crucial for ensuring its accuracy and reliability in predicting PM2.5 emissions. This section delves into the methodology employed for model training, the rationale behind the choice of certain parameters, and the metrics used to evaluate the model's performance.

### 4.4.4 Description of k-fold cross-validation

K-fold cross-validation is a robust method for evaluating the performance of a predictive model. It involves partitioning the original training dataset into k equal-sized subsets, using k - 1 subsets for training and the remaining subset for validation. This process is repeated k times (the folds), with each of the k subsets used exactly once as the validation data. The k results from the folds can then be averaged to produce a single estimation of model performance. This method provides a better understanding of the model's performance by assessing its effectiveness on different subsets of data.

### 4.4.5 The training process, including the choice of the number of epochs

The training of the neural network was performed over a defined number of epochs, where an epoch represents one complete pass through the entire training dataset. The choice of the number of epochs impacts the convergence of the model to a good solution. Too few epochs may result in underfitting, while too many epochs may lead to overfitting. In this study, 250 epochs were chosen based on empirical testing to provide a good balance between training speed and model performance. The training process involves the iterative adjustment of the model's weights to minimize the loss function, which in this case, is the mean squared error between the predicted and actual PM2.5 emissions. The Adam optimization algorithm was employed due to its efficiency and effectiveness in practice. The learning rate, a hyperparameter of the Adam optimizer, was set to 0.01.

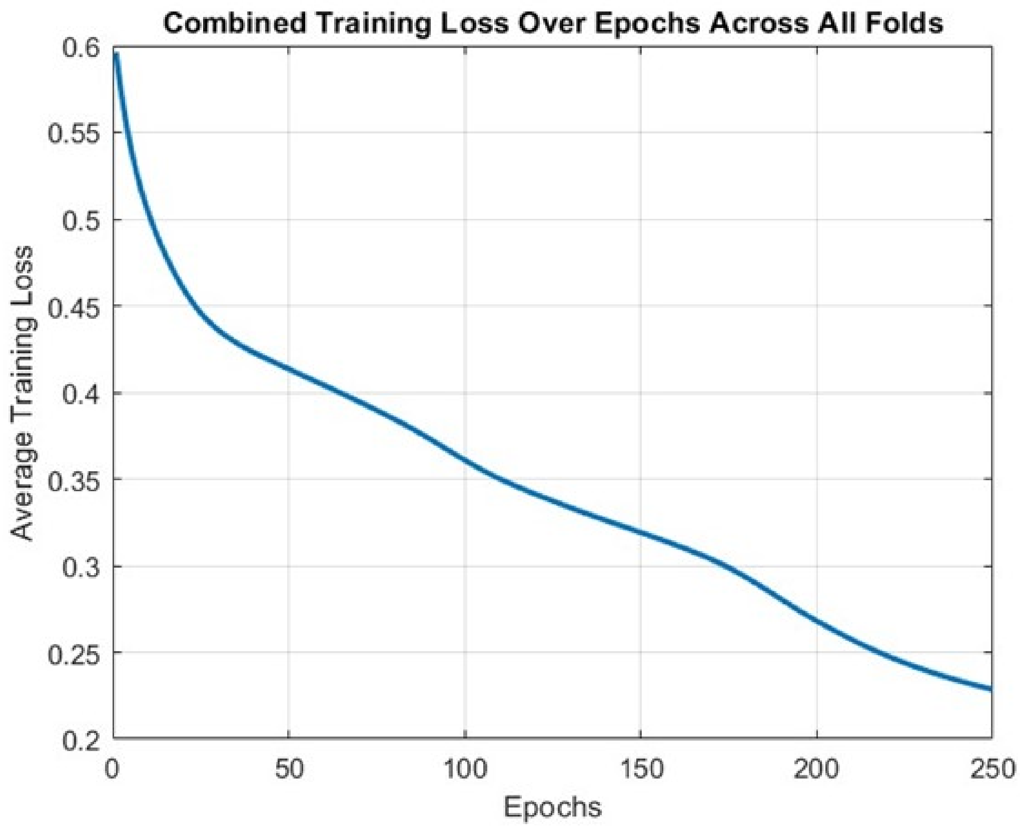


Figure 4.7: Training loss over epochs, showcasing the learning

The graphical representation of the model's training loss over epochs provides a clear visualization of the learning progression. Initially, the training loss starts at a relatively higher level, approximately 0.6, indicative of the model's initial inaccuracy in predicting PM2.5 levels. As the epoch progresses, a significant downward trend in the training loss is observed, settling around 0.23 towards the end. This decline in loss demonstrates the model's improving accuracy and its ability to learn effectively from the training data. The steady decrease in loss across the epochs underscores the efficacy of the chosen network architecture and learning rate, affirming the model's capability to adapt and enhance its predictive performance over time. The final loss value of 0.23 represents a satisfactory level of model training, suggesting that the neural network has successfully captured the underlying patterns in the data without overfitting.

### 4.4.6 progression of the neural network

- Evaluation metrics used to assess the model Evaluating the performance of the model is crucial to ascertain its predictive accuracy and generalization capability. Two common regression metrics were used for this purpose:

- Mean Squared Error (MSE): It measures the average squared differences between the predicted and actual values, giving a rough idea of the magnitude of the error, but not its direction. A lower MSE value indicates a better fit of the model to the data.

- Mean Absolute Error (MAE): It calculates the average absolute differences between the predicted and actual values, which provides a linear error penalty and is more robust to outliers compared to MSE.

Through the 5-fold cross-validation process, I calculated these metrics for each fold and then averaged them to understand the overall performance of the model. The average MSE and MAE values obtained from the validation process were instrumental in assessing the model's accuracy.

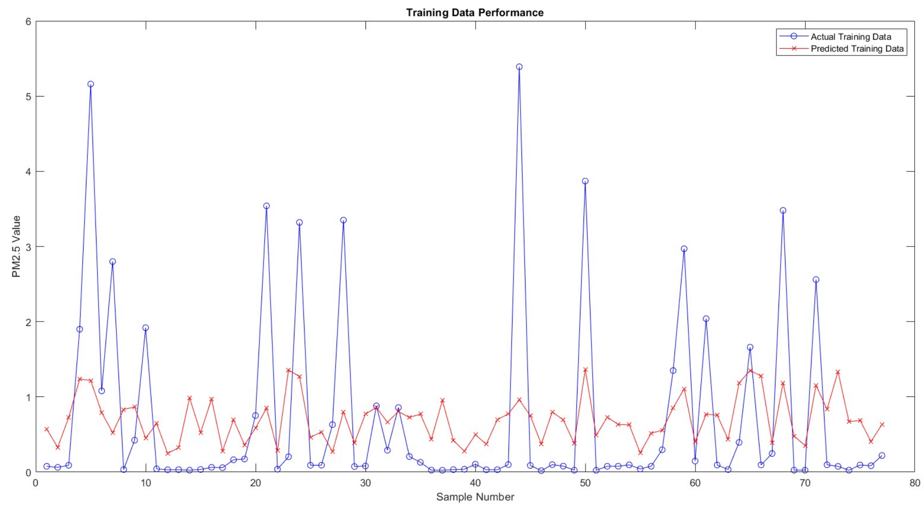


Figure 4.8: Distribution of Errors Showcasing the Model's Prediction Accuracy Across the Dataset(Training set)

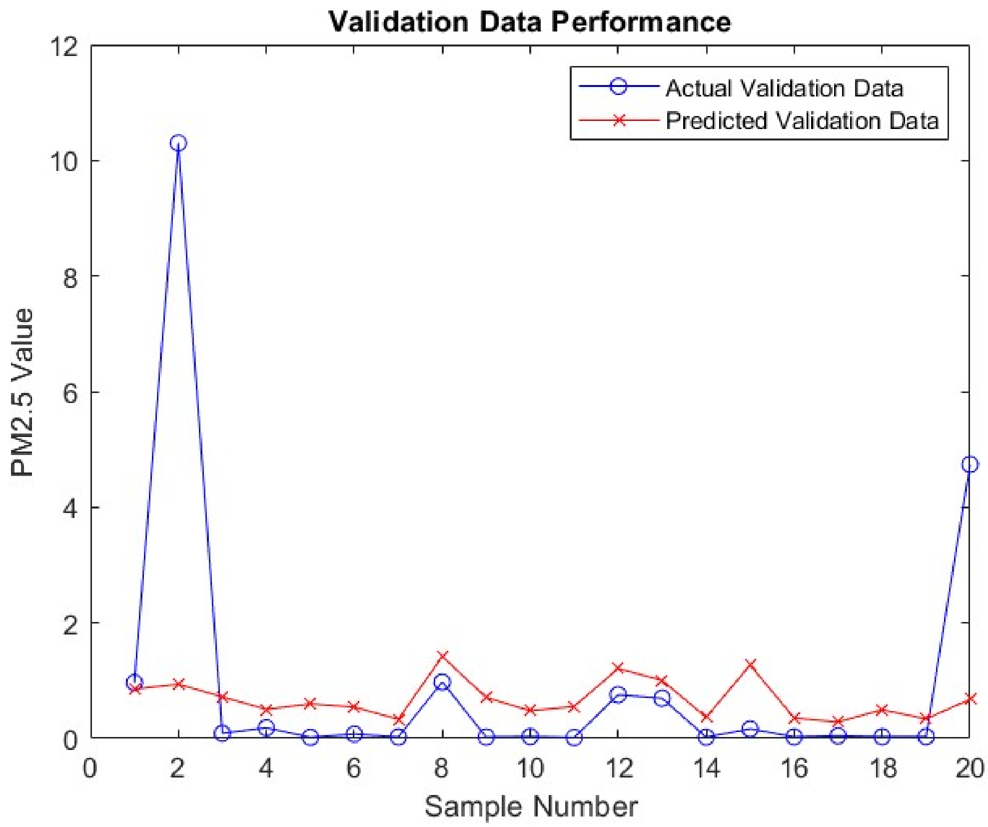


Figure 4.9: Distribution of Errors Showcasing the Model's Prediction Accuracy Across the Dataset(Validation set)

Figure4.8, which presents a plot of the "Actual vs Predicted PM2.5 Values for training Samples," and Figure4.9 which displays the plot for "Actual vs Predicted PM2.5 values for validation Samples" visually demonstrate the model's performance. In these plots, the proximity of the predicted values to the actual PM2.5 values provides a clear representation of the model's accuracy. Additionally, a residual plot, included in the supplementary materials, directly visualizes the distribution of errors, further emphasizing the effectiveness of the MSE and MAE metrics. In the context of the model's performance, the distribution of errors, as illustrated in Figure 4.9, offers insightful perspectives. The spread and central tendency of the error distribution are critical in understanding the reliability and consistency of the model. Areas where the model shows larger errors indicate opportunities for further improvement and refinement. These metrics provide a quantitative measure of the model's ability to predict PM2.5 emissions accurately. Through meticulous training and validation, a reliable model was developed, which demonstrated satisfactory predictive accuracy on unseen data.

## 4.5 Results and Discussion

This section encompasses the presentation of the results obtained from the training and validation of the neural network model. The performance of the model is critically analyzed, and a comparative discussion is carried out to benchmark against baseline models or previous work in the domain.

### 4.5.1 Presentation of the model's performance on training and validation data

The performance of the neural network model was evaluated using the mean squared error (MSE) and mean absolute error (MAE) metrics on both the training and validation data. The results are presented in the following table:

Table 4.1: Performance metrics of the neural network model on training and validation data

| Metric | Training data | Validation data |
|---|---|---|
| MSE | 0.91 | 0.61 |
| MAE | 0.64 | 0.56 |

The training process's progression was also visualized by plotting the training loss across epochs, as shown in Figure 4.7 This figure illustrates the convergence of the model towards a minimum loss point, indicating learning from the data. The distribution of errors, as demonstrated in Figure 4.8, provides insight into the model's prediction accuracy across the dataset. The results indicate a satisfactory performance of the neural network model in predicting PM2.5 emissions. The neural network exhibits superior or comparable performance, showcasing its potential for practical deployment in almond harvesting operations. The key advantages of the developed neural network model include its ability to capture nonlinear relationships in the data and its capability to generalize well to unseen data, courtesy of the k-fold cross-validation employed during training. However, the model's performance could be further enhanced with a larger dataset or by exploring more sophisticated neural network architectures and training methodologies. Additionally, the model could be extended to predict other forms of particulate matter emissions or optimized for real-time monitoring and prediction in an industrial setting. The user interface developed facilitates easy utilization of the model by end-users, making the transition from theory to practice seamless. The findings from this work lay a solid foundation for future research in the domain of environmental monitoring and control in agricultural operations, specifically focusing on reducing particulate matter emissions during harvesting. This section presents a detailed analysis of the results, offering a comprehensive understanding of the model's performance and its comparative advantages over other methodologies. The discussion also paves the way for future research avenues, highlighting the significance of this work in bridging the gap between academic research and practical application.

### 4.5.2 Interactive Prediction Interface

The culmination of this project is the development of an interactive prediction interface that allows users to input new data and receive predictions for PM2.5 emissions. This section delves into the design and utility of this interactive interface, emphasizing its potential for practical deployment.

### 4.5.3 Description of the interactive interface for making new predictions

The interactive prediction interface was developed to facilitate ease of use and accessibility for individuals looking to estimate PM2.5 emissions based on new input data. Upon executing the code, a dialog box prompts the user to input the values for the horizontal brush speed, the angular velocity of the vertical brushes, and the forward speed of the harvester. These inputs are then fed into the trained neural network model, which outputs the predicted PM2.5 emissions. The interface leverages MATLAB's built-in functions, such as inputdlg to create dialog boxes for user input and msgbox to display the predicted PM2.5 values.

### 4.5.4 Discussion on how this interface can be used for practical purposes

The developed interactive prediction interface stands as a bridge between the theoretical model and practical utility. It allows for real-time estimation of PM2.5 emissions, which is crucial for monitoring and controlling air quality during almond harvesting operations. The straightforward and user-friendly design ensures that individuals with varying levels of technical expertise can utilize the model to make informed decisions. Moreover, the interface could be integrated into a more comprehensive monitoring system, allowing for automated data collection and analysis. This could significantly enhance the efficiency and effectiveness of environmental monitoring and control measures. This interactive interface also sets a precedent for the development of similar predictive tools in agriculture and other industries where monitoring and controlling particulate matter emissions are crucial. By providing a tangible means for stakeholders to leverage the predictive model, this interface plays a pivotal role in translating academic research into practical solutions that contribute to sustainable agricultural practices. The development and deployment of the interactive prediction interface epitomizes the practical application of the research conducted in this project. By facilitating the real-time prediction of PM2.5 emissions, this interface significantly contributes to the advancement of environmental monitoring and control measures in almond harvesting operations and beyond.

## 4.6 Conclusion and Future Work

The endeavor to design a Neural Network model for predicting PM2.5 emissions from a newly developed almond harvesting machine has indeed been a venture of acquiring deeper insights into the dynamics of machine operations and their environmental implications. The following sections summarize the key findings, discuss the implications of this work, and propose recommendations for future endeavors in this domain.

### 4.6.1 Summary of Key Findings

- Correlation between PM2.5 and PM10: A significant correlation was discovered between PM2.5 and PM10 emissions, which justified the utilization of only PM2.5 for modeling purposes. This simplifies the model and reduces the computational resources required for training and predictions.

- Outlier Removal and Data Normalization: Employing outlier removal and data normalization techniques significantly improved the quality of the dataset, rendering it suitable for training a neural network.

- Neural Network Performance: The neural network, with its specified architecture, exhibited satisfactory performance in predicting PM2.5 emissions based on the three input parameters: horizontal brush speed, angular velocity of the sweepers, and forward speed of the machine.

- K-fold Cross-validation: Utilizing k-fold cross-validation ensured a more robust evaluation of the model's performance, reducing the risk of overfitting.

- Interactive Prediction Interface: The interactive interface designed for making new predictions enhances the practical utility of the model, allowing for real-time predictions of PM2.5 emissions based on user-input machine parameters.

- Implications of the Work The success of this project holds notable implications for both the academic and practical realms. It bridges the gap between theoretical understanding and practical application of machine learning in predicting emissions from agricultural machinery. Moreover, it sets a precedent for environmental responsibility by attempting to quantify and predict emissions from agricultural operations. From a practical standpoint, this work lays the groundwork for developing smart, self-monitoring agricultural machinery that can provide real-time feedback on emissions, enabling operators to adjust machine parameters on the fly to minimize environmental impact.

### 4.6.2 Recommendations for Future Work in This Area

- Expanding Dataset: Collecting more data under a variety of operational conditions and environments would improve the robustness and generalizability of the model.

- Advanced Model Architectures: Exploring more advanced neural network architectures and other machine learning models could potentially yield better predictive accuracy.

- Feature Engineering: Further analysis could be conducted to identify additional features that may improve the model's predictive power.

- Real-time Monitoring System: Developing a real-time monitoring system integrated with the neural network model could provide continuous feedback to operators, promoting environmentally responsible operation of the machine.

- Comparative Studies: Conducting comparative studies with other emission prediction models to evaluate the relative performance and identify areas for improvement.

- Policy Implications: Investigating the policy implications of this work could also be a fruitful avenue for future research, especially in the context of environmental regulations governing agricultural emissions.

This chapter encapsulates the methodology, findings, and implications of utilizing a neural network model to predict PM2.5 emissions from a novel almond harvester. It not only contributes to the academic discourse on machine learning applications in agriculture but also holds practical implications for the development of environmentally responsible agricultural machinery.

# Chapter 5

# RESULTS AND DISCUSSION

## 5.1 Introduction

This chapter presents a detailed analysis of the field tests conducted to compare the dust generation from different almond pickup machines, including the model developed as part of this research and various commercial alternatives. The primary focus is on the particulate matter sizes PM10 and PM2.5, which are crucial indicators of air quality and health impact. This analysis aims to provide insights into the operational efficiency of these machines in terms of dust emissions and to evaluate the environmental impact of almond harvesting processes.

## 5.2 Measurement Methodology

The measurement of dust particles during the field tests was conducted using the DustTrak DRX (Model Number: 8533), a reliable and accurate device for monitoring air quality.

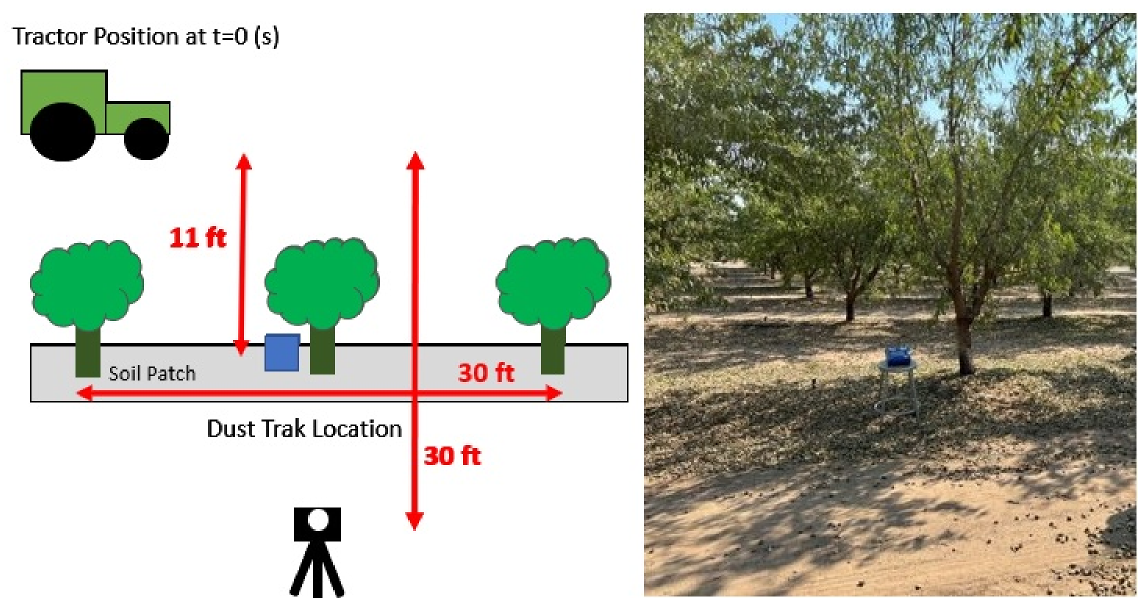


Figure 5.1: DustTrak positioning for dust generation measurement

The location of DustTrak is next to the middle tree, and the test starts from the first tree to the third tree.

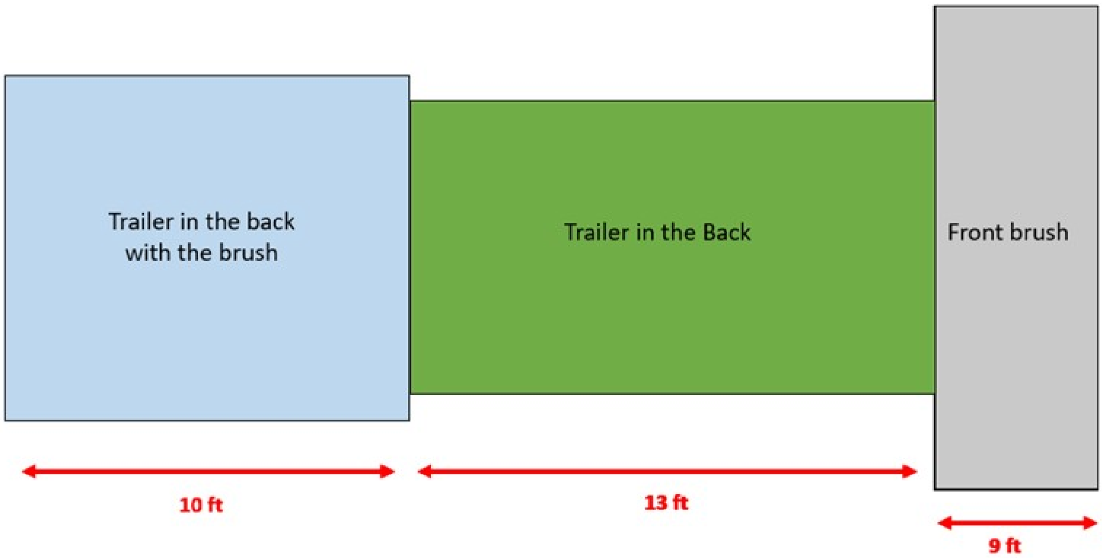


Figure 5.2: Tractor schematic dimension

### 5.2.1 DustTrak Positioning and Setup

- Location: The DustTrak was strategically placed next to a middle tree within the test area, which spanned from the first tree to the third tree. This positioning was chosen to optimally capture dust emissions during the operation of the almond pickup machines.
- Distance Measurements: The device was positioned 30 feet away from two significant points in the test area, ensuring a balanced coverage of the dust dispersion. Additionally, it was placed 11 feet from another reference point, likely the initial position of the tractor, to closely monitor dust emissions at the source.
- Environmental Conditions: Each test accounted for environmental factors such as temperature, wind speed and direction, humidity, and other relevant conditions, as these can significantly influence dust generation and distribution.
- Operational Parameters: The tests were conducted under various operational settings, including different speeds and configurations of the almond pickup machines. These parameters were carefully controlled and documented to provide a comprehensive assessment of their impact on dust emissions. In the next section, I will present and analyze the data collected from the field tests, starting with the dust generation by commercial machines.

## 5.3 Analysis of Dust Generation by Commercial Machines

In this section, I will analyze the dust generation data collected for the Flory 58 Series, Flory 8770, and Weiss McNair machines. The focus is on measuring the concentrations of PM10, indicative of different scales of particulate matter.

- Flory 58 Series (Sweeper): The data for the Flory 58 Series sweeper showed significant variations in PM10 level. The PM10 levels peaked at a specific point (15 mg/m3), suggesting operational conditions that might lead to heightened dust emissions.


Figure 5.3: Flory 58 series non-cab nut sweeper [11]

Analysis of the PM2.5 data provides insights into the finer particulate matter emissions, which have direct health implications due to their ability to penetrate deeply into the respiratory system.

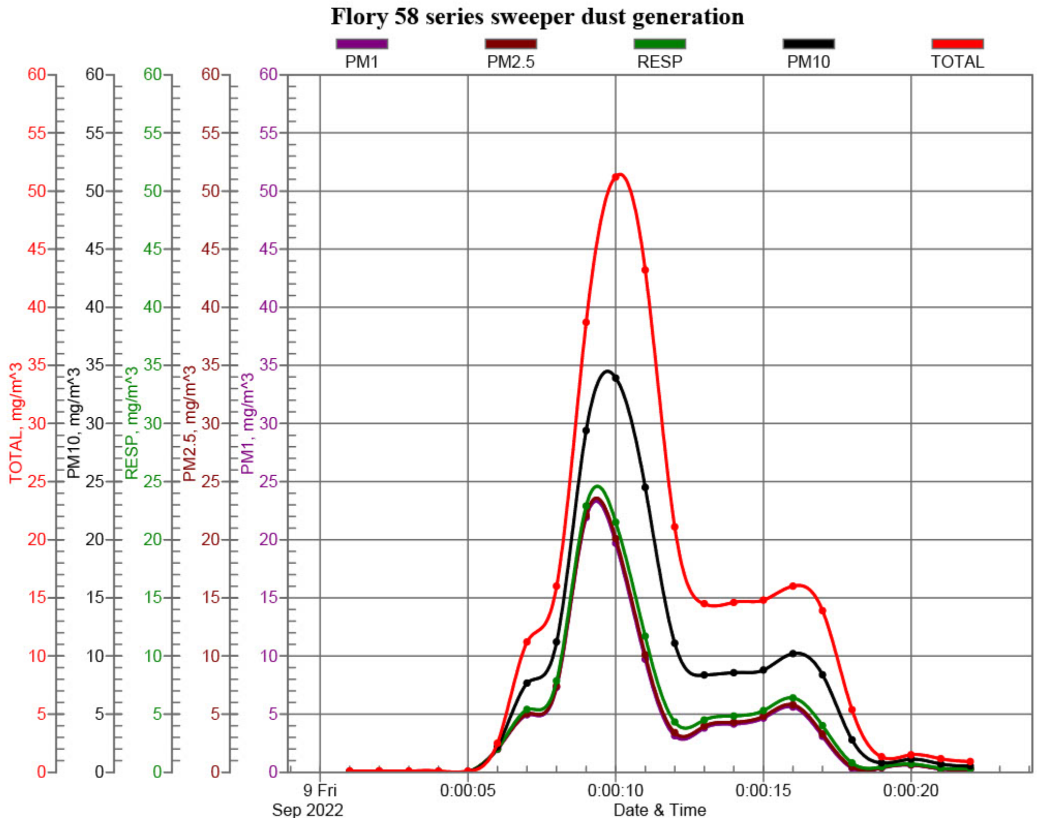


Figure 5.4: Flory 58 series sweeper dust generation in one round

In Figure5.4, total dust generation is displayed and we focus on PM10 as a comparing factor as other parameters are correlated with PM10.

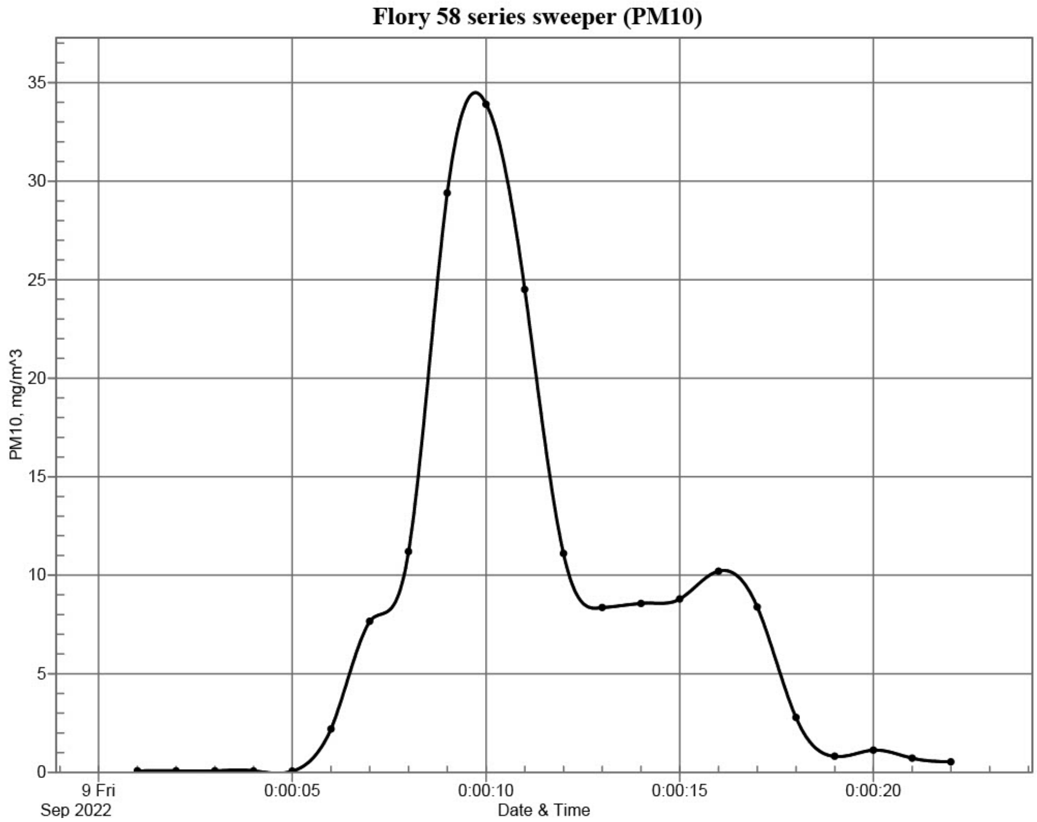


Figure 5.5: PM10 generation for Flory 58 Series sweeper

- Flory 8770 (Pickup machine): For the Flory 8770 machine, the maximum PM10 level was observed to be around 150 mg/m$^3$, indicating a potential for significant dust generation under certain operational conditions.

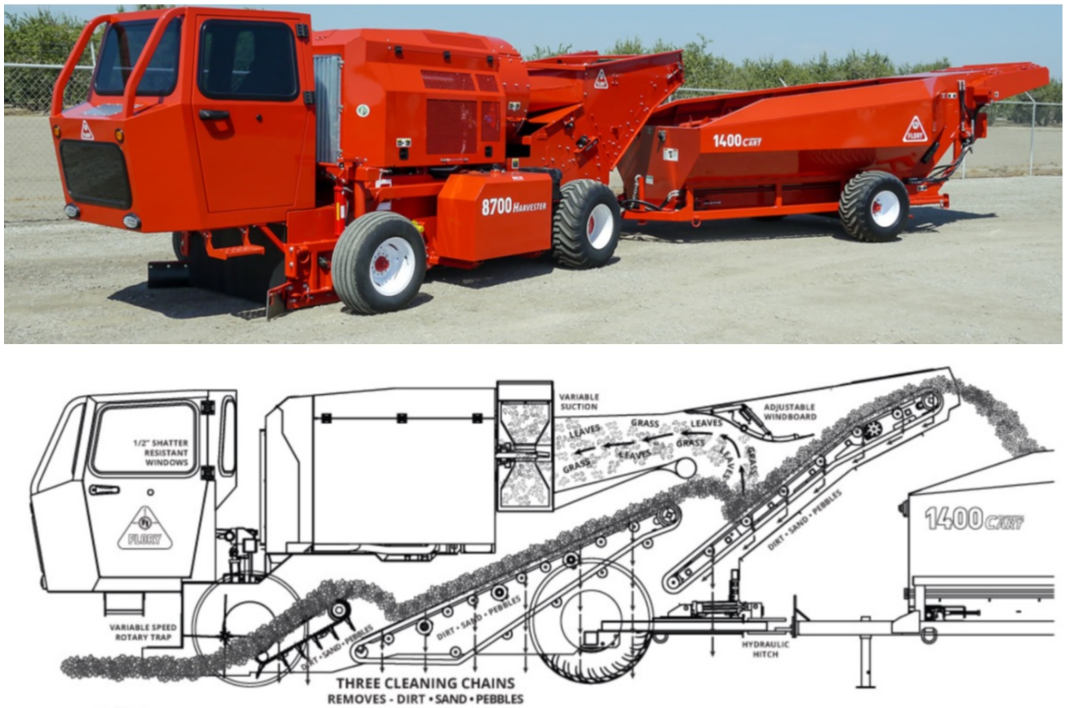


Figure 5.6: Flory 8770 pickup machine [24]

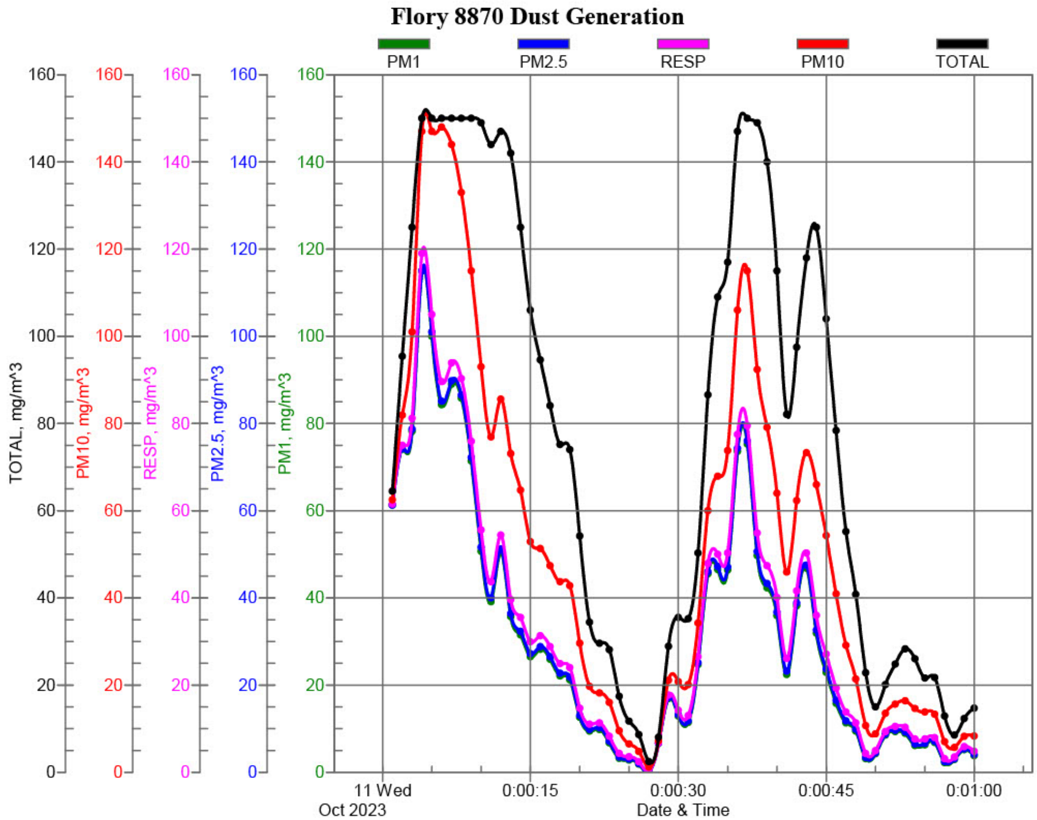


Figure 5.7: Flory 8770 pickup machine dust generation

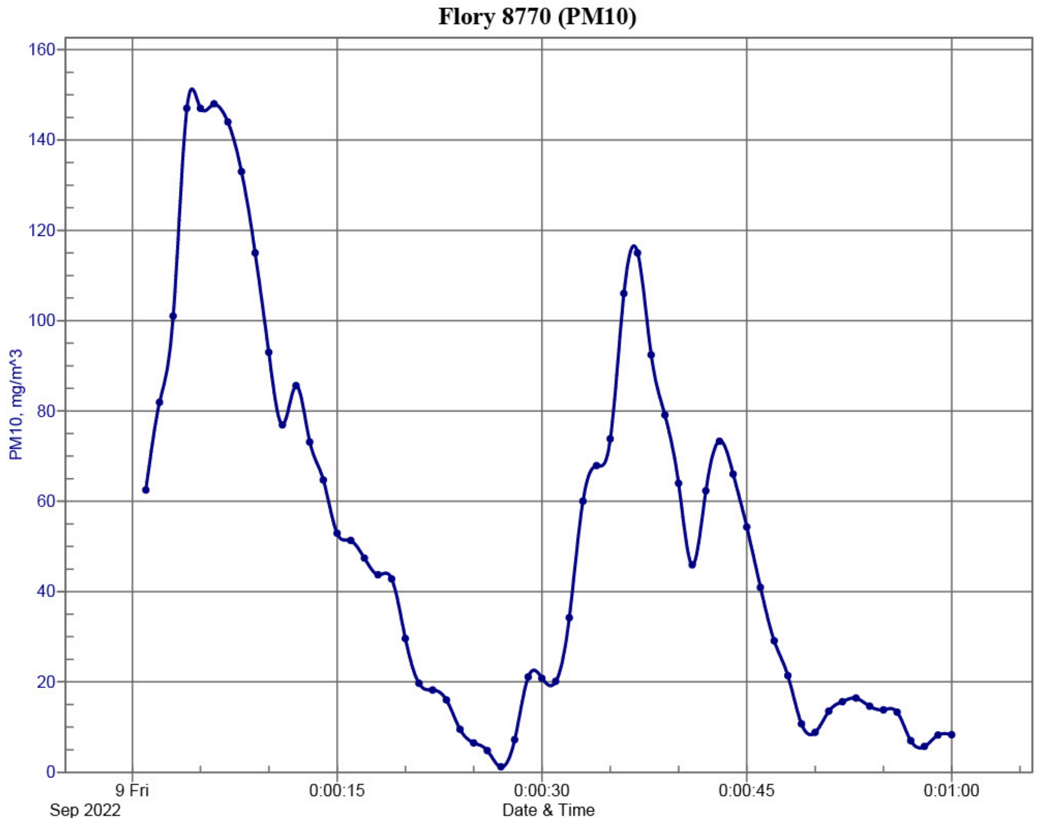


Figure 5.8: PM10 generation for Flory 8770 pickup machine

The PM10 concentration data similarly showed elevated levels, necessitating a discussion on the potential environmental and health impacts.

- Weiss McNair 9810 pickup machine: The Weiss McNair machine also exhibited high dust emissions, with PM10 reaching similar maximum levels as the Flory 8770. The PM2.5 data from this machine complemented the findings for PM10, providing a comprehensive understanding of its dust emission profile.


Figure 5.9: Weiss McNair 9810 pickup machine [25]

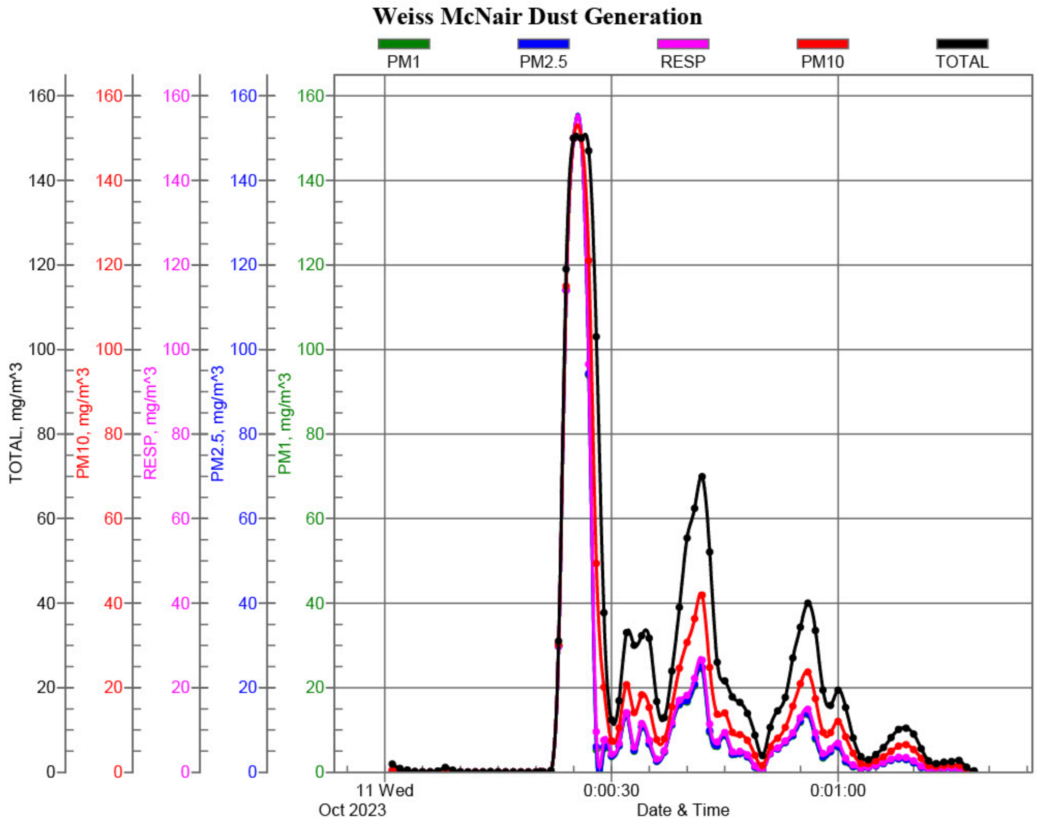


Figure 5.10: Weiss McNair 9810 pickup machine dust generation

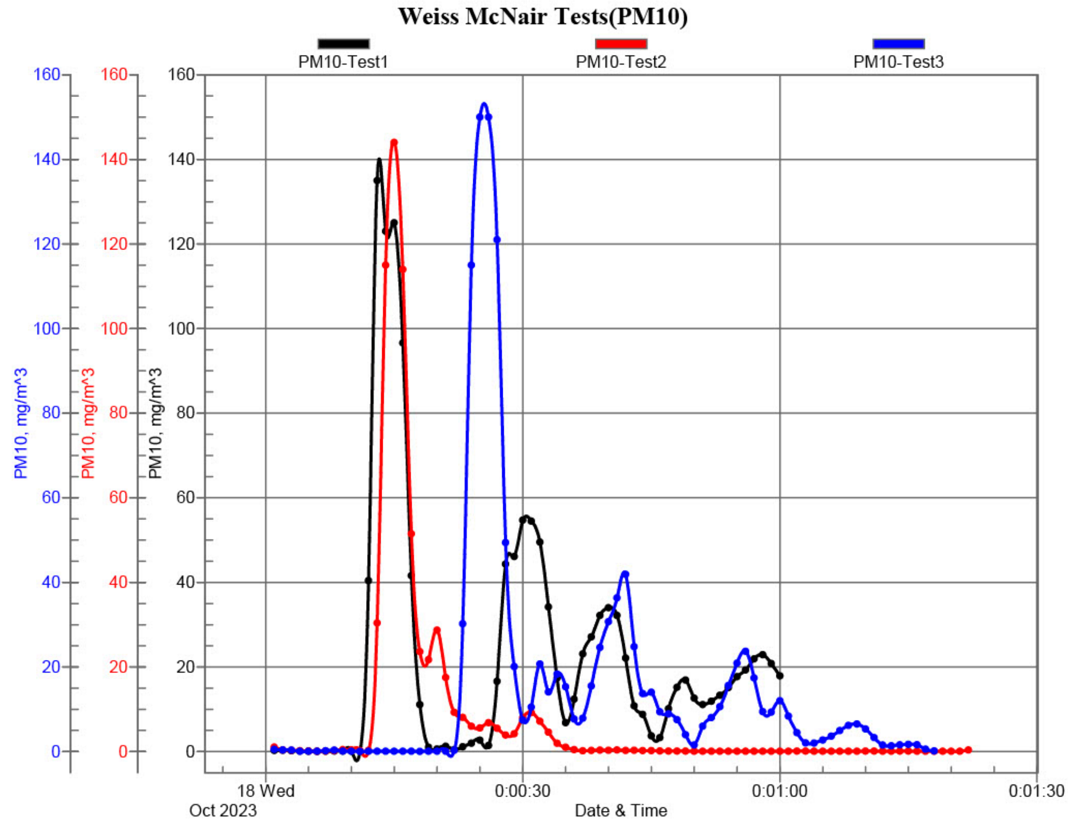


Figure 5.11: PM10 generation for Weiss McNair 9810 pickup machine

## 5.4 Comparison of commercial machines and our new machine

This section compares the dust emissions of the commercial machines with the final design of the almond pickup machine developed in this research.

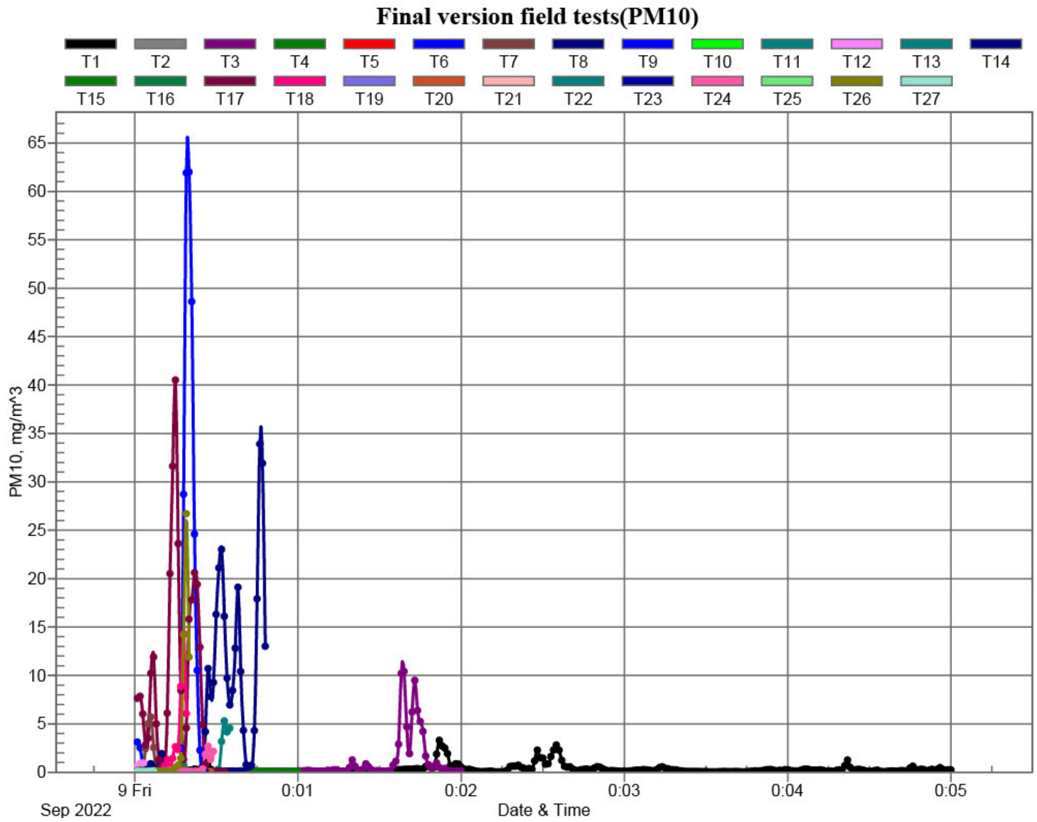


Figure 5.12: PM10 generation of our new combined sweeper and pickup machine

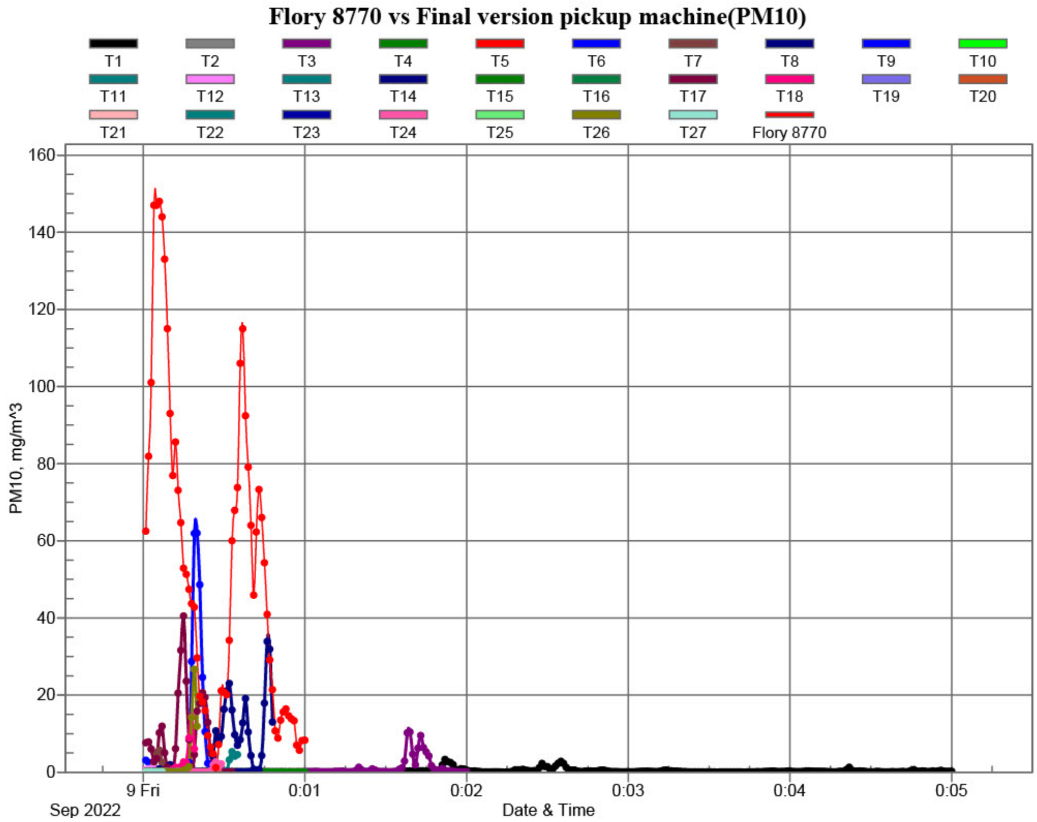


Figure 5.13: PM10 generation comparison between Flory 8770 and our new pickup machine

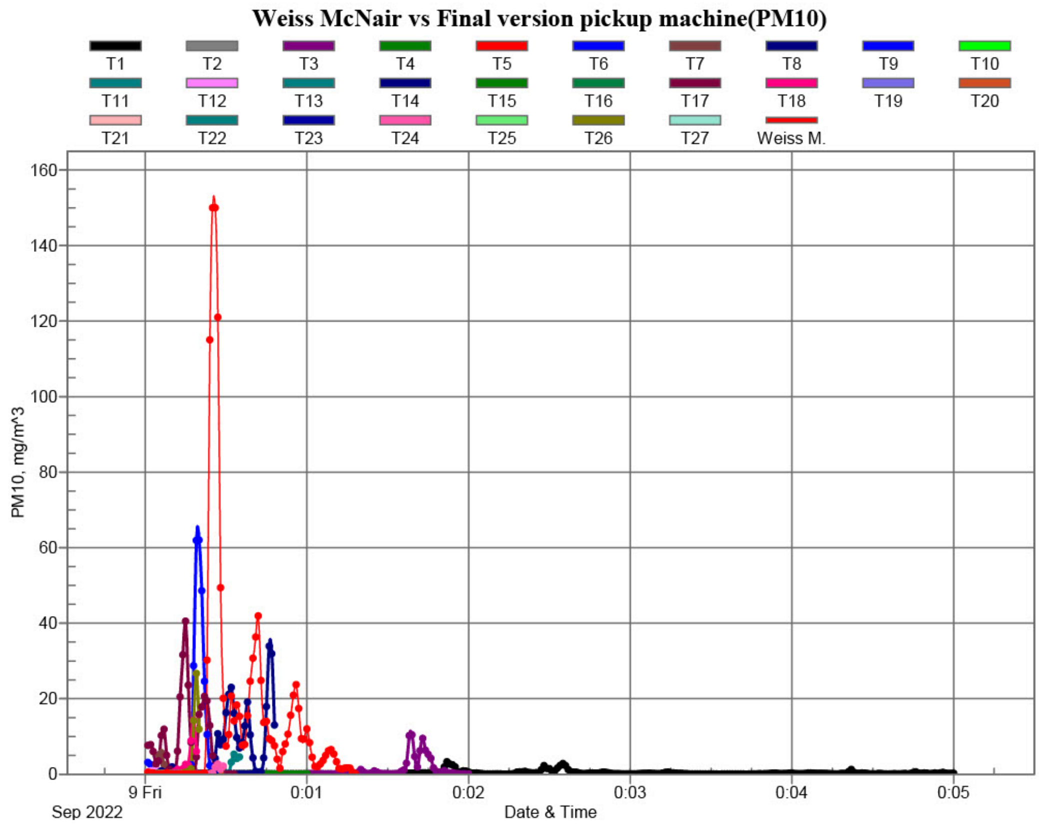


Figure 5.14: PM10 generation comparison between Weiss McNair 9810 and our new pickup machine

- Comparative Analysis (PM10): In contrast to the commercial machines, the PM10 levels from the final version of the designed machine did not exceed 65 mg/m$^3$ in any of the 27 field tests. This stark difference highlights the effectiveness of the design in significantly reducing PM10 emissions.

- PM2.5 Analysis: Similarly, the PM2.5 levels for the designed machine were consistently lower than those of the commercial alternatives, further emphasizing the environmental and health advantages of the new design.

## 5.5 Environmental and Health Implications

### 5.5.1 The findings from the field tests have substantial implications for the environment and health

- Reduced Dust Emissions: The significantly lower PM10 and PM2.5 levels from the designed machine indicate a reduced potential for air pollution and associated health risks.

- Sustainable Almond Harvesting: The data supports the potential of the new machine design to contribute to more sustainable almond harvesting practices, with a lower environmental footprint.

## 5.6 Operational Insights

### 5.6.1 An analysis of the operational conditions during the tests reveals

Influence of Operational Settings: Different operational settings, such as the speed and configuration of the machines, had varying impacts on dust emissions. This insight is crucial for optimizing machine operations to minimize environmental impact.

### 5.6.2 Implications for Commercial Machines

The findings suggest areas for potential improvements in existing commercial machines to reduce their environmental impact.

## 5.7 Concluding Remarks

This chapter presented a comprehensive analysis of the dust emissions from various almond pickup machines. The significantly lower dust emissions recorded for the newly designed machine compared to commercial alternatives underscore its potential for more environmentally friendly almond harvesting.

## 5.8 Future Work

Future research could focus on:

- Further Optimization: Continuing to refine the design of the almond pickup machine to enhance its operational efficiency and environmental sustainability.
- Broader Applications: Exploring the application of the principles and technologies developed in this research to other agricultural machinery and contexts.

# Chapter 6

# CONCLUSION

## 6.1 Fulfillment of Research Objectives

This thesis embarked on a mission to innovate almond harvesting processes, with specific objectives tailored towards integrating technology and environmental sustainability. The successful integration of the sweeping and pickup steps into a singular, efficient process marks a significant advancement in almond harvesting operations. We engineered an optimal mechanism that prioritizes the minimization of dust generation, addressing a critical environmental concern in agricultural practices. A key achievement of this research was the development of an automated feedback control system. This system not only maximizes the efficiency of almond sweeping from the ground but also plays a pivotal role in minimizing dust generation through reduced soil contact. The implementation of this system demonstrates the practicality and effectiveness of automation in agricultural machinery. Furthermore, the application of predictive neural network modeling stands as a cornerstone of this research. This innovative approach allowed for real-time estimation and control of dust generation, harnessing the power of data analytics and machine learning. The success of this modeling technique in predicting dust levels under various operational conditions is a testament to the potential of integrating advanced computational methods in agricultural practices. The comparative performance evaluations conducted between the developed almond pickup and sweeper systems and existing commercial machines emphasized the effectiveness of our design in reducing dust emissions. This comprehensive analysis not only validated the technological advancements but also highlighted the environmental benefits of our system.

## 6.2 Environmental and Health Impacts

The environmental and health implications of this research are profound and multifaceted. By significantly reducing dust emissions, the newly developed almond pickup machine makes a substantial contribution to improving air quality. This is particularly crucial in almond harvesting regions, where dust is not merely a byproduct of agricultural processes but a significant environmental hazard. The reduction in particulate matter emissions is a vital step toward mitigating respiratory problems and other health risks associated with poor air quality. This is especially beneficial for agricultural workers and nearby communities who are most vulnerable to these risks. Additionally, the reduction in dust emissions aligns with global efforts to combat climate change and environmental degradation, reinforcing the critical role of sustainable agricultural practices in preserving ecological balance.

## 6.3 Technological Advancements and Operational Efficiency

This research has led to significant technological advancements in almond harvesting. The integration of sweeping and pickup processes into a unified, efficient operation demonstrates a leap in agricultural machinery design. The automation of dust control, a notable achievement of this research, showcases the practical application of advanced technology in real-world agricultural settings. The use of predictive neural network modeling is particularly groundbreaking. This model exemplifies the potential of artificial intelligence and machine learning in optimizing agricultural practices, paving the way for smarter, more efficient farming techniques. These innovations not only improve operational efficiency but also set new benchmarks for environmental sustainability in agriculture, proving that technological progress can be a powerful ally in the quest for ecological conservation.

## 6.4 Comparative Analysis with Commercial Machines

Comparative analysis with commercial machines has been a cornerstone of this research, providing clear evidence of the superiority of the new design. The almond pickup machine developed in this thesis outperforms commercial alternatives in crucial aspects, most notably in dust control. This achievement is not just a technical victory but a significant environmental milestone. By offering a more environmentally friendly solution to almond harvesting, this machine sets a new standard in the industry. It challenges the status quo and demonstrates that it is possible to achieve high operational efficiency without compromising environmental health. This comparative analysis underscores the importance of continuous innovation in agricultural machinery to meet both production and environmental goals.

## 6.5 Challenges, Limitations, and Future Directions

Despite the significant achievements, this research encountered challenges and limitations that provide valuable lessons and opportunities for future work. One of the primary challenges was balancing technological sophistication with practicality and cost-effectiveness. The complexities involved in integrating advanced systems like neural networks into everyday farming operations also presented considerable challenges. Future research should focus on further optimizing the machine design, particularly in terms of scalability and user-friendliness. Exploring alternative materials and technologies that could enhance the machine's environmental footprint and efficiency is also recommended. Additionally, expanding testing under varied environmental conditions would provide more comprehensive data on the machine's performance. A promising direction for future research is the broader application of the technology and techniques developed in this thesis, potentially extending to other types of agricultural machinery and practices. This future work could further solidify the role of technological innovation as a key driver in the evolution of sustainable agriculture.

### 6.6 Concluding Remarks

- Reflection on Broader Implications for Sustainable Agricultural Practices: This research transcends beyond the technical realm of almond harvesting; it embodies a broader commitment to sustainable agricultural practices. The journey undertaken in this thesis highlights the pivotal role of technological innovation in addressing environmental challenges. By successfully integrating sweeping and pickup steps, and meticulously engineering a mechanism that prioritizes minimal dust generation, this work sets a precedent for environmental stewardship in agriculture. The development of an automated feedback control system stands as a testament to the power of technology in enhancing efficiency while conscientiously reducing environmental impact. These advancements underscore a crucial narrative - that technological progress and environmental sustainability are not mutually exclusive, but rather, they are synergistic. The application of predictive neural network modeling further demonstrates how cutting-edge technology can be harnessed to make real-time, data-driven decisions that significantly curb the ecological footprint of farming practices. In essence, this thesis is not just about creating a more efficient almond pickup machine; it is about reimagining agricultural practices through the lens of sustainability and innovation.

- Vision for the Future of Almond Harvesting: Looking forward, the vision for almond harvesting is one where efficiency and environmental health are intrinsically interwoven. The potential for widespread adoption of the practices and technologies developed in this research is vast. Imagine fields where almond harvesting is seamlessly conducted with minimal dust emission, where the air quality remains uncompromised, and where the health of the community and the environment is upheld as a paramount concern. As this research paves the way, it is envisaged that similar sustainable approaches will be embraced across various facets of agriculture. The future beckons a paradigm shift - from conventional practices to methods that are ecologically sound and technologically advanced. This thesis is a step towards that future, a future where almond harvesting not only yields bountiful crops but also nurtures the health of our planet and its inhabitants.

# Bibliography


[1] United States Department of Agriculture. *USDA Statistics by State for California*. 2021. URL: https://www.nass.usda.gov/Statistics_by_State/California/index.php (visited on 2021).

[2] *California Almond Forecast*. 2022. URL: https://www.almonds.com/sites/default/files/2021-05/2021SubjectiveForecast.pdf (visited on 2022).

[3] C. Koehnen. *Harvesting Techniques*. 2020. URL: https://www.koehnen.com/harvesting (visited on 2020).

[4] J. Cox. *Almond Industry Weighs Measures for Cutting Harvest-Related Air Pollution*. 2020. URL: https://www.bakersfield.com/news/almond-industry-weighs-measures-for-cutting-harvest-related-air-pollution/article_2c0bc2b8-d031-11ea-8e37-0b1376463416.html (visited on 2020).

[5] Almond Board of California. *Orchard Management: Harvest Dust Reduction*. URL: https://www.almonds.com/almond-industry/orchard-management/harvest/dust-reduction.

[6] J. Underhill. *Air Pollutants of Primary Concern*. URL: https://www4.des.state.nh.us/appc/?page_id=138.

[7] L. M. Randolph. *Inhalable Particulate Matter and Health (PM2.5 and PM10)*. 2012. URL: https://ww2.arb.ca.gov/resources/inhalable-particulate-matter-and-health (visited on 2012).

[8] T. Frantz. *'Clearing the Air': Dust*. 2017. URL: https://fresnoalliance.com/dust/ (visited on 2017).

[9] *Exact Harvester: An Exciting New Standard in Low Dust Nut Harvesting*. 2018. URL: https://exactcorp.com/products/conditioners/e-250-e-z-prep-conditioner/ (visited on 2018).

[10] Jackrabbit. *Lower Dust, Cleaner Product, Faster Speed*. 2019. URL: https://jackrabbitequipment.com/harvester/ (visited on 2019).

[11] Flory. *Flory Industries - PTO Nut Harvester*. 2019. URL: https://www.goflory.com/index.php/products/item/860-pto-nut-harvester/.

[12] W. McNair. *Weiss McNair*. 2019. URL: https://www.weissmcnair.com/.

[13] Y. Xie and A. Alleyne. “Two Degree of Freedom Control Synthesis with Applications to Agricultural Systems”. In: *Journal of Dynamic Systems, Measurement, and Control* 136.5 (2014), pp. 1–11.

[14] R. Yang et al. “The Design and Experimentation of EVPIVS-PID Harvesters’ Header Height Control System Based on Sensor Ground Profiling Monitoring”. In: *Agriculture* 12.282 (2022), p. 24.

[15] Y. Xie et al. “Header Height Control of a Combine Harvester System”. In: *Proceedings of the ASME 2010 Dynamic Systems and Control Conference*. Cambridge, MA, USA, 2010.

[16] Y. Ni et al. “Computational model and adjustment system of header height of soybean harvesters based on soil-machine system”. In: *Computers and Electronics in Agriculture* 183 (2021). ISSN: 0168-1699.

[17] Y. Xie et al. “Fundamental Limits in Combine Harvester Header Height Control”. In: *Journal of Dynamic Systems, Measurement, and Control* 135 (2013).

[18] W. Al Sawafi and K. Hassan Ali. “A Fuzzy Adaptive PID Controller Design for Header Height Tracking Control of Agricultural Combine Harvester”. In: *Journal of Mechanical Engineering Research and Developments* 44 (2021), pp. 227–238.

[19] P. Tulpule and A. Kelkar. “Integrated Robust Optimal Design (IROD) of Header Height Control System for Combine Harvester”. In: *Proceedings of the American Control Conference*. Portland, OR, USA, 2014.

[20] L. Zhao et al. “Ground surface detection method using ground penetrating radar signal for sugarcane harvester base-cutter control”. In: *Biosystems Engineering* 219 (2022), pp. 103–123.

[21] X. Xie and A. Alleyne. “A Robust Two Degree-Of-Freedom Controller for Systems with Delay”. In: *Proceedings of the American Control Conference (ACC)*. Conference held on 17–19 June 2013. Washington, DC, USA, June 2013.

[22] X. Lei et al. “Optimal design of one-rotor orchard inter-row rake 220 based on tines trajectory analysis”. In: *International Agricultural Engineering Journal* 28.4 (2019).

[23] Almond Conference. *Almond Orchard 2025: Reducing Dust at Harvest*. 2018. URL: `https://www.almonds.com/sites/default/files/content/attachments/Almond%20Orchard%202025%20Reducing%20Dust%20at%20Harvest.pdf` (visited on 12/06/2018).

[24] Flory Industries. *Flory 850 Low Dust Harvester*. URL: `https://www.goflory.com/index.php/products/item/860-pto-nut-harvester`.

[25] Weiss McNair. *Weiss McNair 9800 California Special*. URL: https://www.weissmcnair.com/9800p-harvester.

[26] Jackrabbit Equipment. *Lower Dust Cleaner Product Faster Speed*. URL: https://jackrabbitequipment.com/harvester/.

[27] California Air Resources Board. *California's 2007-2014 Progress in Reducing PM2.5 and PM10 Emissions from Agricultural Operations and Other Sources*. 2015. URL: https://ww2.arb.ca.gov/emission-inventory-activities (visited on 2015).

[28] S. C. C. and A. L. M. El Jirie N. Baticados. "Particulate Matter Emission Factors Using Low-Dust Harvesters for Almond Nut-Picking Operations". In: *Journal of the Air Waste Management Association* 69.11 (2019), pp. 1304–1311.

[29] S. Altikat. "Prediction of CO2 Emission from Greenhouse to Atmosphere with Artificial Neural Networks and Deep Learning Neural Networks". In: *International Journal of Environmental Science and Technology* 18 (2021), pp. 3169–3178.

[30] D. V. Y. K. Pranali K. Kosamkar. "Analysis and Prediction of Greenhouse Gas Emission Using Feedforward Neural Network". In: *IT in Industry* 9.1 (2021).

[31] A. Kolasa-Wiecek. "Neural Modeling of Greenhouse Gas Emission from Agricultural Sector in European Union Member Countries". In: *Water, Air, Soil Pollution* 229.205 (2018).

[32] S. Chowdhury. "Application of Artificial Neural Network for Predicting Agricultural Methane and CO2 Emissions in Bangladesh". In: *Proceedings of the 12th International Conference on Computing Communication and Networking Technologies (ICCCNT)* 87 (2021), p. 5.

[33] B. K. et al. "Application of Artificial Neural Networks for Prediction of Output Energy and GHG Emissions in Potato Production in Iran". In: *Agricultural Systems* 123 (2014), pp. 120–127.

[34] OSHA Training Library on Silica. *OSHA Training Library on Silica*. URL: https://www.osha.gov/training/library/silica/handout.

[35] EPA Agriculture News. *EPA Agriculture News 2016*. 2016. URL: https://www.epa.gov/agriculture/agriculture-news-2016 (visited on 2016).

[36] B. S. S. et al. "Dust Influenced by Conventional and Undercutter Tillage within the Columbia Plateau, USA". In: *Earth Surface Processes* 34 (2009), pp. 1323–1332.

[37] K. W. Y. Han. "A Review of Artificial Neural Network Techniques for Environmental Issues Prediction". In: *Journal of Thermal Analysis and Calorimetry* 145 (2021), pp. 2191–2207.

[38] I. C. T. P. Alexander Poznyak. "A Survey on Artificial Neural Networks Application for Identification and Control in Environmental Engineering: Biological and Chemical Systems with Uncertain Models". In: *Annual Reviews in Control* 48 (2019), pp. 250–272.

[39] M. B. J. H. R. M. Mohamed A. Shahin. "Recent Advances and Future Challenges for Artificial Neural Systems in Geotechnical Engineering Applications". In: *Advances in Artificial Neural Systems* (2009), p. 9.

[40] B. Iglewicz and H. D. Iglewicz. *How to Detect and Handle Outliers*. ASQ Quality Press, 1993.

[41] A. K. D. R. P. W. and M. J. Jain. "Statistical Pattern Recognition: A Review". In: *IEEE Transactions on Pattern Analysis and Machine Intelligence* 22.1 (2000), pp. 4–37.

[42] C. A. Pope and D. W. Dockery. "Health Effects of Fine Particulate Air Pollution: Lines that Connect". In: *Journal of the Air Waste Management Association* 56.6 (2006), pp. 709–742.

[43] Y. Zhang and T. S. Zhang. "Global Atmospheric Emission Inventory of Polycyclic Aromatic Hydrocarbons (PAHs) for 2004". In: *Atmospheric Environment* 43.4 (2004), pp. 812–819.